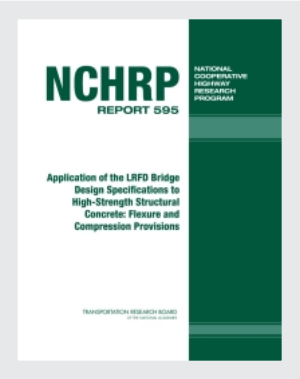

Application of the LRFD Bridge Design Specifications to High-Strength Structural Concrete: Flexure and Compression Provisions

DETAILS

28 pages | | PAPERBACK
ISBN 978-0-309-42489-9 | DOI 10.17226/23269

AUTHORS

NATIONAL COOPERATIVE HIGHWAY RESEARCH PROGRAM

NCHRP REPORT 595

Application of the LRFD Bridge Design Specifications to High-Strength Structural Concrete: Flexure and Compression Provisions

Sami Rizkalla
North Carolina State University
Raleigh, NC

Amir Mirmiran
Florida International University
Miami, FL

Paul Zia
North Carolina State University
Raleigh, NC

Henry Russell
Henry G. Russell, Inc.
Chicago, IL

AND

Robert Mast
Berger/ABAM Engineers, Inc.
Seattle, WA

Subject Areas
Bridges, Other Structures, and Hydraulics and Hydrology

Research sponsored by the American Association of State Highway and Transportation Officials
in cooperation with the Federal Highway Administration

TRANSPORTATION RESEARCH BOARD

WASHINGTON, D.C.
2007
www.TRB.org

NATIONAL COOPERATIVE HIGHWAY RESEARCH PROGRAM

Systematic, well-designed research provides the most effective approach to the solution of many problems facing highway administrators and engineers. Often, highway problems are of local interest and can best be studied by highway departments individually or in cooperation with their state universities and others. However, the accelerating growth of highway transportation develops increasingly complex problems of wide interest to highway authorities. These problems are best studied through a coordinated program of cooperative research.

In recognition of these needs, the highway administrators of the American Association of State Highway and Transportation Officials initiated in 1962 an objective national highway research program employing modern scientific techniques. This program is supported on a continuing basis by funds from participating member states of the Association and it receives the full cooperation and support of the Federal Highway Administration, United States Department of Transportation.

The Transportation Research Board of the National Academies was requested by the Association to administer the research program because of the Board's recognized objectivity and understanding of modern research practices. The Board is uniquely suited for this purpose as it maintains an extensive committee structure from which authorities on any highway transportation subject may be drawn; it possesses avenues of communications and cooperation with federal, state and local governmental agencies, universities, and industry; its relationship to the National Research Council is an insurance of objectivity; it maintains a full-time research correlation staff of specialists in highway transportation matters to bring the findings of research directly to those who are in a position to use them.

The program is developed on the basis of research needs identified by chief administrators of the highway and transportation departments and by committees of AASHTO. Each year, specific areas of research needs to be included in the program are proposed to the National Research Council and the Board by the American Association of State Highway and Transportation Officials. Research projects to fulfill these needs are defined by the Board, and qualified research agencies are selected from those that have submitted proposals. Administration and surveillance of research contracts are the responsibilities of the National Research Council and the Transportation Research Board.

The needs for highway research are many, and the National Cooperative Highway Research Program can make significant contributions to the solution of highway transportation problems of mutual concern to many responsible groups. The program, however, is intended to complement rather than to substitute for or duplicate other highway research programs.

NCHRP REPORT 595

Project 12-64
ISSN 0077-5614
ISBN: 978-0-309-09905-9
Library of Congress Control Number 2007907024

COPYRIGHT PERMISSION

NOTICE

The project that is the subject of this report was a part of the National Cooperative Highway Research Program conducted by the Transportation Research Board with the approval of the Governing Board of the National Research Council. Such approval reflects the Governing Board's judgment that the program concerned is of national importance and appropriate with respect to both the purposes and resources of the National Research Council.

The members of the technical committee selected to monitor this project and to review this report were chosen for recognized scholarly competence and with due consideration for the balance of disciplines appropriate to the project. The opinions and conclusions expressed or implied are those of the research agency that performed the research, and, while they have been accepted as appropriate by the technical committee, they are not necessarily those of the Transportation Research Board, the National Research Council, the American Association of State Highway and Transportation Officials, or the Federal Highway Administration, U.S. Department of Transportation.

Each report is reviewed and accepted for publication by the technical committee according to procedures established and monitored by the Transportation Research Board Executive Committee and the Governing Board of the National Research Council.

The Transportation Research Board of the National Academies, the National Research Council, the Federal Highway Administration, the American Association of State Highway and Transportation Officials, and the individual states participating in the National Cooperative Highway Research Program do not endorse products or manufacturers. Trade or manufacturers' names appear herein solely because they are considered essential to the object of this report.

Published reports of the

NATIONAL COOPERATIVE HIGHWAY RESEARCH PROGRAM

are available from:

Transportation Research Board
Business Office
500 Fifth Street, NW
Washington, DC 20001

and can be ordered through the Internet at:

http://www.national-academies.org/trb/bookstore

Printed in the United States of America

THE NATIONAL ACADEMIES

Advisers to the Nation on Science, Engineering, and Medicine

The **National Academy of Sciences** is a private, nonprofit, self-perpetuating society of distinguished scholars engaged in scientific and engineering research, dedicated to the furtherance of science and technology and to their use for the general welfare. On the authority of the charter granted to it by the Congress in 1863, the Academy has a mandate that requires it to advise the federal government on scientific and technical matters. Dr. Ralph J. Cicerone is president of the National Academy of Sciences.

The **National Academy of Engineering** was established in 1964, under the charter of the National Academy of Sciences, as a parallel organization of outstanding engineers. It is autonomous in its administration and in the selection of its members, sharing with the National Academy of Sciences the responsibility for advising the federal government. The National Academy of Engineering also sponsors engineering programs aimed at meeting national needs, encourages education and research, and recognizes the superior achievements of engineers. Dr. Charles M. Vest is president of the National Academy of Engineering.

The **Institute of Medicine** was established in 1970 by the National Academy of Sciences to secure the services of eminent members of appropriate professions in the examination of policy matters pertaining to the health of the public. The Institute acts under the responsibility given to the National Academy of Sciences by its congressional charter to be an adviser to the federal government and, on its own initiative, to identify issues of medical care, research, and education. Dr. Harvey V. Fineberg is president of the Institute of Medicine.

The **National Research Council** was organized by the National Academy of Sciences in 1916 to associate the broad community of science and technology with the Academy's purposes of furthering knowledge and advising the federal government. Functioning in accordance with general policies determined by the Academy, the Council has become the principal operating agency of both the National Academy of Sciences and the National Academy of Engineering in providing services to the government, the public, and the scientific and engineering communities. The Council is administered jointly by both the Academies and the Institute of Medicine. Dr. Ralph J. Cicerone and Dr. Charles M. Vest are chair and vice chair, respectively, of the National Research Council.

The **Transportation Research Board** is one of six major divisions of the National Research Council, which serves as an independent adviser to the federal government and others on scientific and technical questions of national importance. The National Research Council is jointly administered by the National Academy of Sciences, the National Academy of Engineering, and the Institute of Medicine. The mission of the Transportation Research Board is to provide leadership in transportation innovation and progress through research and information exchange, conducted within a setting that is objective, interdisciplinary, and multimodal. The Board's varied activities annually engage about 7,000 engineers, scientists, and other transportation researchers and practitioners from the public and private sectors and academia, all of whom contribute their expertise in the public interest. The program is supported by state transportation departments, federal agencies including the component administrations of the U.S. Department of Transportation, and other organizations and individuals interested in the development of transportation. **www.TRB.org**

www.national-academies.org

CRP STAFF FOR NCHRP REPORT 595

Christopher W. Jenks, *Director, Cooperative Research Programs*
Crawford F. Jencks, *Deputy Director, Cooperative Research Programs*
David B. Beal, *Senior Program Officer*
Eileen P. Delaney, *Director of Publications*
Hilary Freer, *Senior Editor*

NCHRP PROJECT 12-64 PANEL
Field of Design—Area of Bridges

Harry A. Capers, Jr., *Arora and Associates, P.C., Lawrenceville, NJ* (Chair)
John M. Holt, *Texas DOT, Austin, TX*
Elmer Marx, *Alaska DOT, Juneau, AK*
Richard Miller, *University of Cincinnati, Cincinnati, OH*
Michael R. Pope, *California DOT, Sacramento, CA*
Jerry L. Potter, *Livingston, TX*
Samia Shaaban, *Shaaban Engineering, Newark, NJ*
Joey Hartmann, *FHWA Liaison*
Stephen F. Maher, *TRB Liaison*

AUTHOR ACKNOWLEDGMENTS

The research documented herein has been performed under NCHRP Project 12-64 by the Department of Civil, Construction, and Environmental Engineering at North Carolina State University; Department of Civil and Environmental Engineering at Florida International University; Henry G. Russell, Inc.; and Berger/ABAM Engineers, Inc. North Carolina State University is the prime contractor for this study. The work undertaken at Florida International University, Henry G. Russell, Inc., and Berger/ABAM Engineers, Inc., are through separate subcontracts with North Carolina State University.

Sami Rizkalla, Distinguished Professor of Civil and Construction Engineering at the North Carolina State University, is the principal investigator. Co-Principal Investigators of this project are Amir Mirmiran, Professor and Chair of the Department of Civil and Environmental Engineering at Florida International University, and Paul Zia, Distinguished University Professor Emeritus at North Carolina State University. Consultants for the project are Henry G. Russell, Vice President of Henry G. Russell, Inc., and Robert Mast, Senior Principal, Berger/ABAM Engineers, Inc. Graduate students who participated in this project are Halit Cenan Mertol, Zhenhua Wu, Wonchang Choi, SungJoong Kim, and Andrew Logan.

FOREWORD

By David B. Beal
Staff Officer
Transportation Research Board

This report documents research performed to develop recommended revisions to the *AASHTO LRFD Bridge Design Specifications* to extend the applicability of the flexural and compression design provisions for reinforced and prestressed concrete members to concrete strengths greater than 10 ksi. The report details the research performed and includes recommended revisions to the *Specifications*. The material in this report will be of immediate interest to bridge designers.

The *AASHTO LRFD Bridge Design Specifications* state: "Concrete strengths above 10.0 ksi shall be used only when physical tests are made to establish the relationships between the concrete strength and other properties." When the LRFD specifications were written, the data were insufficient to demonstrate that the provisions were applicable to concrete compressive strengths above 10 ksi (high-strength concrete). Nevertheless, recent research has started to address design issues with high-strength concrete, and the FHWA Showcase Projects are encouraging the use of high-strength concrete in bridge structures. There is a need to expand the LRFD specifications to allow greater use of high-strength concrete.

The objective of this research was to develop recommended revisions to the *AASHTO LRFD Bridge Design Specifications* to extend the applicability of flexural and compression design provisions for reinforced and prestressed concrete members to concrete strengths greater than 10 ksi. Companion NCHRP Projects 12-56 (published as *NCHRP Report 579*) and 12-60 (publication pending) address shear and transfer and development length, respectively.

This research was performed by North Carolina State University, Florida International University, Henry G. Russell, Inc., and Berger/ABAM Engineers. The report fully documents the research leading to the recommended revisions to Section 5 of the *AASHTO LRFD Bridge Design Specifications*.

CONTENTS

CHAPTER 1

Introduction

1.1 Problem Statement

The AASHTO LRFD Bridge Design Specifications (*1*), first published in 1994, includes an article (5.4.2.1) limiting its applicability to maximum concrete strength of 10 ksi (69 MPa), unless physical tests are made to establish the relationship between concrete strength and its other properties. This limitation was imposed because of the lack of research data when the specifications were developed. Many design provisions stipulated in the LRFD Specifications are still based on test results obtained from specimens with compressive strengths up to 6 ksi (41 MPa). Although such a strength limit is not explicitly imposed by other codes such as the ACI 318-05 (*2*), except in its provisions for shear and development length, their applicability to high-strength concrete (HSC) is not fully addressed either. Since the first publication of the LRFD Specifications in 1994, the use of HSC in bridges has increased significantly and more research information has become available.

1.2 Research Objective

The NCHRP issued four separate projects to extend the LRFD Specifications to allow broader use of HSC and to meet the needs of the bridge design community. NCHRP Project 18-07 addressed prestress losses in pretensioned concrete girders (Tadros et al. [*3*]). NCHRP Project 12-56 addressed shear and NCHRP Project 12-60 addressed bond and development length in reinforced and prestressed concrete, respectively. The objective of this NCHRP Project 12-64 was to develop recommended revisions to the LRFD Specifications (*1*) to extend the applicability of its flexural and compression design provisions for reinforced and prestressed concrete members for concrete strengths up to 18 ksi (124 MPa). Ideally, the recommended provisions should be seamless and unified over the full range of concrete strengths.

1.3 Research Approach

The project began on August 15, 2003, and was extended through April 30, 2007. The following tasks were performed:

1. The existing research and practice regarding flexural and compressive behavior and design of reinforced and prestressed HSC members were reviewed. Based on collected information, factors that affect the flexural and compressive behavior and design of reinforced and prestressed HSC members were determined. Additional research needed to extend the LRFD Specifications to HSC was identified.
2. A detailed experimental research program was conducted to evaluate the material properties of HSC, flexural and compressive behavior of reinforced HSC members, and flexural behavior of prestressed HSC members.
3. Test results were obtained, evaluated, and compiled with the results available in the literature. Based on the analyses of these results, recommended revisions to the LRFD Specifications were developed to extend the applicability of its compressive and combined compressive and flexural design provisions to concrete with compressive strengths up to 18 ksi (124 MPa).

1.4 Report Organization

This report consists of four chapters and seven appendixes. This chapter serves as an introduction, describes the problem statement, defines the objectives, and outlines the research approach in this project. Chapter 2 provides the findings based on the test results of this project, as well as other researches reported in the literature. Proposed equations and design guidelines to extend the LRFD Specifications to include HSC up to 18 ksi (124 MPa) are also presented.

Chapter 3 summarizes the proposed provisions to the LRFD Specifications. Finally, conclusions and recommendations for future research are presented in Chapter 4. Detailed information about the testing program, test results, and analyses related to material properties, distribution of stresses in the compression zone of flexural members, beams under flexure and axial-flexural loadings, columns under concentric and eccentric loading, and prestressed girders are given in Appendixes A, B, C, D, and E, respectively. Proposed revisions to the LRFD Specifications are presented in Appendix F. For future reference, Appendix G contains all relevant experimental data developed and assembled in this research project. All appendixes are available for downloading from the NCHRP project website.

CHAPTER 2

Research Findings

2.1 Introduction

This chapter briefly outlines the research program and describes the research findings that served as the basis for the recommended revisions to the LRFD Specifications (*1*) to extend the applicability of its compressive and flexural design provisions for concrete with compressive strengths up to 18 ksi (124 MPa). The experimental programs that were performed include tests for material properties; flexural, axial-compression, and combined axial and flexure tests for reinforced concrete members; and flexural tests for prestressed concrete members.

2.2 Material Properties

A total of 321 specimens of different sizes and shapes were tested to determine the material characteristics of HSC, including compressive strength, elastic modulus, modulus of rupture, creep, and shrinkage of concrete with target compressive strengths ranging from 10 ksi to 18 ksi (69 to 124 MPa). The variables investigated in this study were concrete strength, specimen size, curing process, age of loading, and stress level. Test set-ups, test results, and findings are summarized below. Detailed discussions of this test program are presented in Appendix A.

2.2.1 Compressive Strength

Compressive strength tests were performed using both 4 × 8 in. (100 × 200 mm) and 6 × 12 in. (150 × 300 mm) cylinders in accordance with AASHTO T 22 (*4*) (ASTM C 39 [*5*]), as shown in Figure 2-1. The 4 × 8 in. (100 × 200 mm) cylinders were tested at ages of 1, 7, 14, 28, and 56 days. The 6 × 12 in. (150 × 300 mm) cylinders were tested at 28 and 56 days. Three different curing conditions were used in this investigation: 1-day heat curing, 7-day moist curing followed by air curing, and continuous moist curing until the time of testing.

Tests results at 28 and 56 days indicate that cylinders moist cured for 7 days, followed by air curing, exhibited the highest compressive strengths among the three different curing methods. On the other hand, 1-day heat curing generally resulted in the lowest strength. Cylinders moist cured up to the time of testing produced strengths slightly lower than the 7-day moist-cured specimens. The strength reduction may be attributed to the differences in internal moisture conditions at the time of testing. Comparisons of the compressive strengths of the 7-day moist-cured and the continuously moist-cured specimens suggested that, for HSC, moist curing beyond 7 days does not result in any significant increase in strength because of the low permeability of HSC and the short time required for the capillary pores to be blocked. Average ratios of compressive strengths of the 4 × 8 in. (100 × 200 mm) to the 6 × 12 in. (150 × 300 mm) cylinders for the 1-day heat-cured, 7-day moist-cured, and continuously moist-cured specimens were 1.05, 1.03, and 1.03, respectively. These ratios indicate that the size effect of HSC cylinders is negligible.

2.2.2 Modulus of Elasticity

ASTM C 469 (*6*) method was followed to determine the elastic modulus using 4 × 8 in. (100 × 200 mm) concrete cylinders as shown in Figure 2-1. The collected data were used to calculate the elastic modulus and the Poisson's ratio.

Tests results, at ages of 28 and 56 days, indicate that the continuously moist-cured cylinders had the highest values of elastic modulus. This result may be attributed to the moist surface conditions at the time of testing.

Based on the results obtained in this research, combined with test results reported in the literature (over 4,400 data points), the following equation is proposed for the modulus of elasticity of concrete up to 18 ksi (124 MPa):

$$E_c(ksi) = 310000K_1\left(w_c(kcf)\right)^{2.5}\cdot\left(f_c'(ksi)\right)^{0.33}$$
$$E_c(MPa) = 0.000035K_1\left(w_c(kg/m^3)\right)^{2.5}\cdot\left(f_c'(MPa)\right)^{0.33} \quad (2\text{-}1)$$

Figure 2-1. Test set-up for compressive strength and elastic modulus.

where K_1 is the correction factor for source of aggregate to be taken as 1.0 unless determined by physical test and as approved by the authority of jurisdiction, w_c is the unit weight of concrete, and f_c' is the specified compressive strength of concrete.

A comparison of predicted modulus of elasticity using Equation 2-1 with the measured modulus of elasticity for the entire 4,400 datapoint database is shown in Figure 2-2. The proposed Equation 2-1 slightly overestimates the data obtained in this research.

The normal distribution of the collected data with respect to the current LRFD Specifications (*1*), ACI 363R-92 (*7*), and the proposed equation are shown in Figure 2-3, in which *P(x)* is the probability function defined as follows:

$$P(x) = \frac{1}{\sigma\sqrt{2\pi}} \exp\left(-\frac{(x-\mu)^2}{2\sigma^2}\right) \quad (2\text{-}2)$$

where σ is the standard deviation, exp is the exponential function, μ is the mean, and x is the variable.

The normal distribution curve for the recommended equation (NCHRP 12-64) shows that the mean of the ratio of the predicted to the measured elastic modulus is closest to 1, although the standard deviation is slightly higher than the one determined by the ACI 363R-92 (*7*) equation.

2.2.3 Modulus of Rupture

The modulus of rupture tests were performed using 6 × 6 × 20 in. (150 × 150 × 500 mm) beam specimens subjected to four-point loading in accordance with AASHTO T 97 (*8*). The test set-up is illustrated in Figure 2-4.

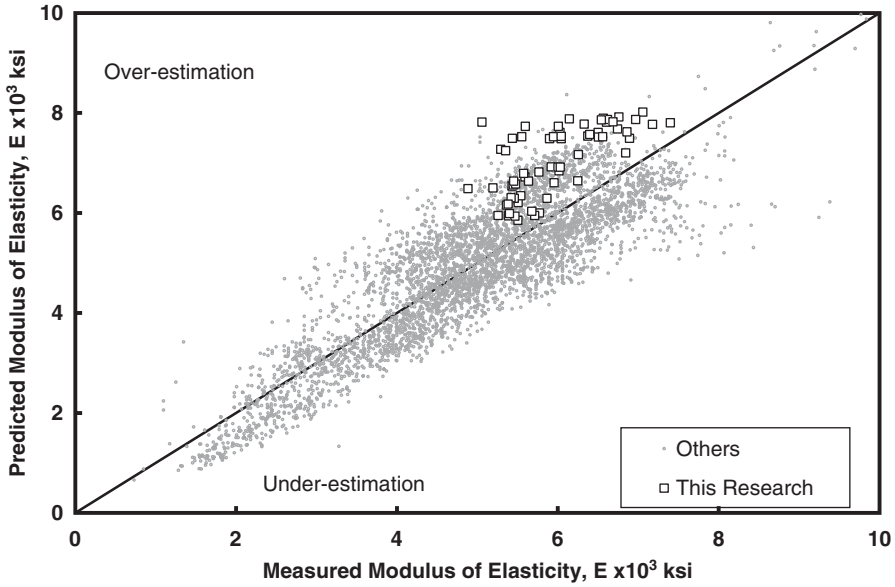

Figure 2-2. Predictions of over 4,400 data points using the proposed equation.

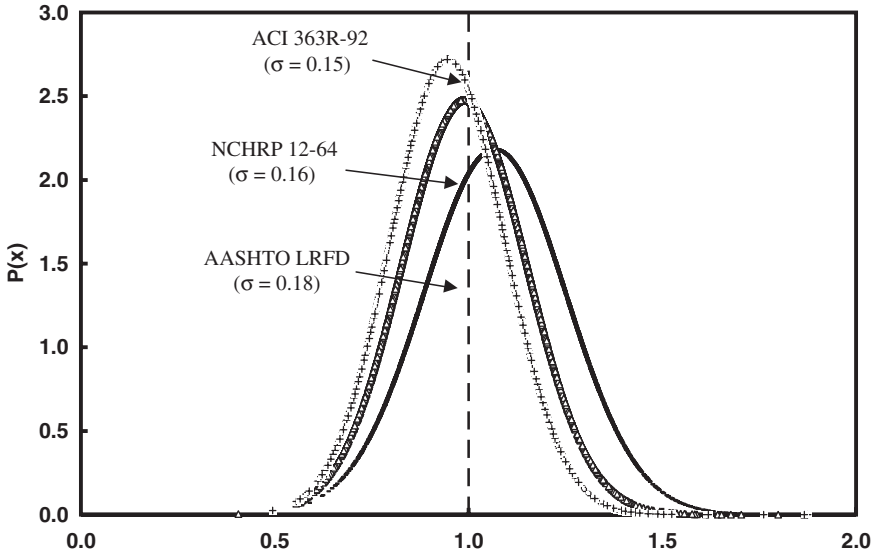

Figure 2-3. Normal distribution for predicted/measured modulus of elasticity.

Figure 2-5 shows the test data from material study (Appendix A), reinforced concrete beams (Appendix C), and prestressed concrete girders (Appendix E) tested in this program along with the data collected from Legeron and Paultre (*9*), Paultre and Mitchell (*10*), Mokhtarzadeh and French (*11*), Li (*12*), and the Noguchi Laboratory (*13*). Two equations for modulus of rupture given in Section 5.4.2.6 of the current LRFD Specifications are also shown in the figure. Some of the tests results correspond better to the current upper bound of the LRFD Specifications. This is mainly because of the curing condition and moisture content of the specimens. Test results suggest that the current lower bound of the LRFD Specifications overestimates the modulus of rupture for HSC. Therefore a better predictive equation, $f_r = 0.19\sqrt{f_c'(ksi)}$ $(f_r = 0.5\sqrt{f_c'(MPa)})$, is proposed for HSC up to 18 ksi (124 MPa).

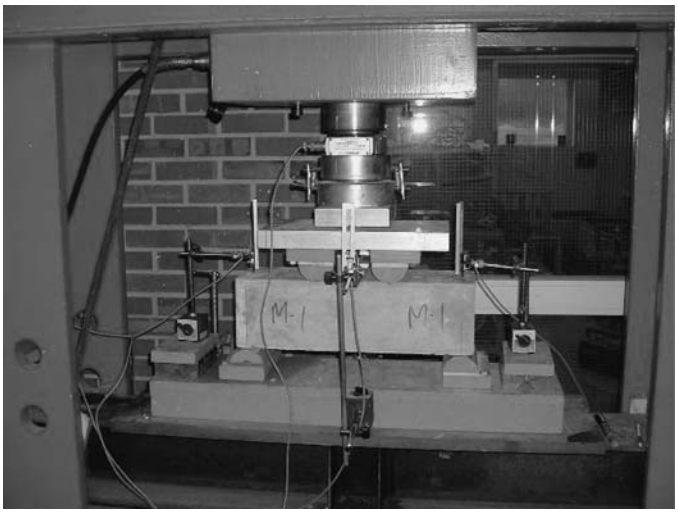

Figure 2-4. Test set-up modulus of rupture.

2.2.4 Poisson's Ratio

Based on the results of the concrete cylinders (Appendix A) and eccentric bracket specimens tested in this program (Appendix B), combined with other research data in the literature, Poisson's ratio of 0.2 was found to be acceptable for concrete compressive strengths up to 18 ksi (124 MPa), as shown in Figure 2-6. Research data from the literature include those obtained by Komendant et al. (*14*), Perenchio and Klieger (*15*), Carrasquillo et al. (*16*), Swartz et al. (*17*), Jerath and Yamane (*18*), Radain et al. (*19*), and Iravani (*20*).

2.2.5 Creep

Creep testing was performed using 4×12 in. (100×300 mm) cylindrical specimens. The test set-up is shown in Figure 2-7. Two identical cylindrical specimens were stacked and loaded in each creep rack. Two different stress levels equivalent to $0.2\,f_c'A_g$ and $0.4\,f_c'A_g$ were used in this study, where f_c' is the target concrete compressive strength and A_g is the gross area of concrete cylinder. One-day heat-cured specimens were loaded at the end of curing, whereas the 7-day moist-cured specimens were loaded at the 7th, 14th, and 28th days. The creep specimens had companion 4×12 in. (100×300 mm) cylindrical shrinkage specimens being used to measure the shrinkage strain.

In general, the test results indicate that the creep behavior of HSC is similar to normal-strength concrete (NSC), where creep rate decreases as time increases. For the same concrete

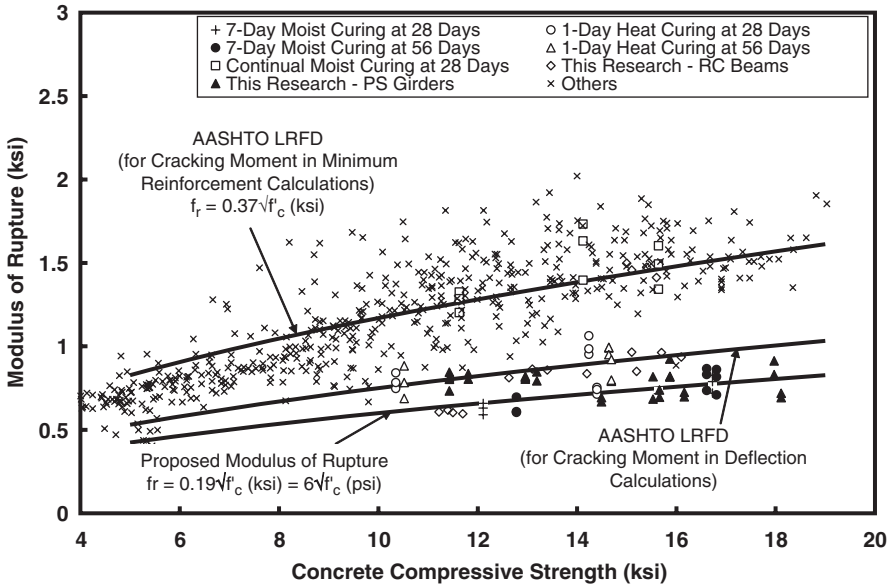

Figure 2-5. Modulus of rupture vs. compressive strength.

strength, the creep of 1-day heat-cured cylinders is less than that of the 7-day moist-cured cylinders. As with NSC, the creep for HSC is proportional to the applied stress, provided that the applied stress is less than the proportional limit.

The relationships specified by the LRFD Specifications were found to be reasonably accurate to predict creep of HSC, except for the time-development correction factor (k_{td}) that produced negative values in the first few days after loading, if the concrete strengths were greater than 15 ksi (103 MPa). Accordingly, the following time-development correction factor was developed to overcome the anomaly associated with the current time-development correction factor:

$$k_{td} = \frac{t}{12\left(\frac{100 - 4f'_{ci}}{f'_{ci} + 20}\right) + t} \quad (f'_{ci} \text{ in ksi})$$

$$k_{td} = \frac{t}{12\left(\frac{100 - 0.58f'_{ci}}{0.145f'_{ci} + 20}\right) + t} \quad (f'_{ci} \text{ in MPa}) \qquad (2\text{-}3)$$

where t is the age of concrete after loading in days and f'_{ci} is the specified compressive strength at prestress transfer for prestressed members or 80 percent of the strength at service for non-prestressed members.

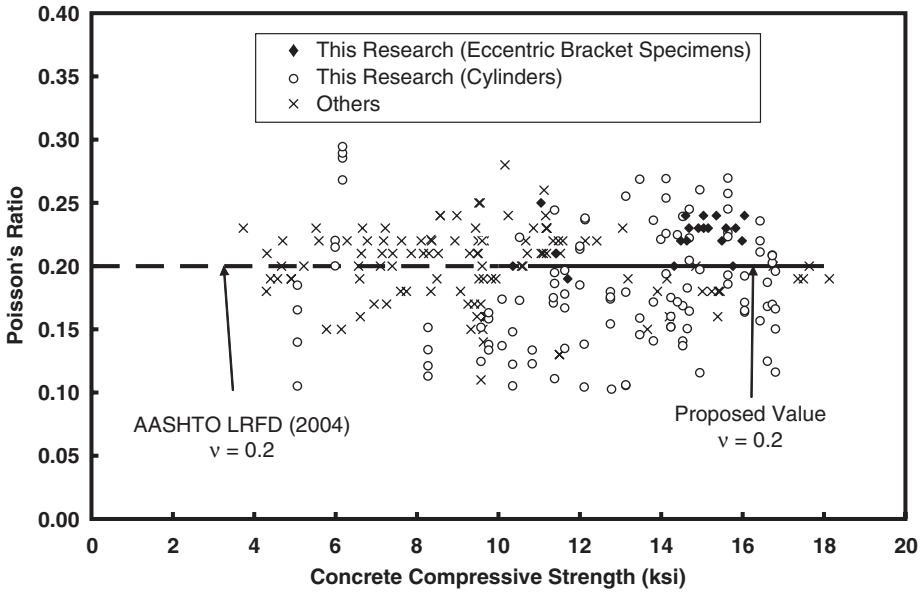

Figure 2-6. Proposed relationship for Poisson's ratio.

Figure 2-7. Test set-up for creep.

In Figure 2-8, the proposed time-development correction factor and the current expression specified by the LRFD Specifications are compared for 8 and 16 ksi (55 and 110 MPa) concrete compressive strengths. More detailed information can be found in Appendix A.

2.2.6 Shrinkage

Prism specimens of 3 × 3 × 11¼ in. (75 × 75 × 280 mm) were used to evaluate shrinkage behavior in accordance with ASTM C 157 (*21*). The test set-up is shown in Figure 2-9. Tests for 1-day heat-cured specimens were started at the end of the first day, whereas tests for 7-day moist-cured specimens were started at the 7th day.

The test results indicate that there was less shrinkage for heat-cured specimens than for moist-cured cylinders. The difference in the shrinkage for HSC specimens with concrete compressive strengths ranging from 10 to 18 ksi (69 and 124 MPa) was fairly small. The test results also indicate that predictions of shrinkage using the LRFD Specifications can be made, provided that the proposed time-development factor (Equation 2-3) is used.

2.3 Flexural Members

This section summarizes the findings from the tests performed to evaluate the flexural behavior of HSC beams at failure. The experimental program consisted of two types of specimens: (1) specially designed eccentric bracket specimens to study the stress-strain distribution in the compression zone of flexural members and (2) reinforced concrete beams to determine the overall behavior of HSC flexural members, including the ultimate compressive strain, cracking moment, and deflection.

2.3.1 Distribution of Compressive Stresses in Compression Zone of Flexural Members

Twenty-one 9 × 9 × 40 in. (225 × 225 × 1000 mm) unreinforced HSC eccentric bracket specimens were subjected to combined axial load and flexure to determine the stress-strain distribution in the compression zone of flexural members. The test concept was based on the method developed by Hognestad et al. (*22*) to simulate the compression zone of a flexural member. The two axial loads were adjusted during the test to maintain zero strain (which represents the neutral axis of a flexural member) at one face of the specimen and the

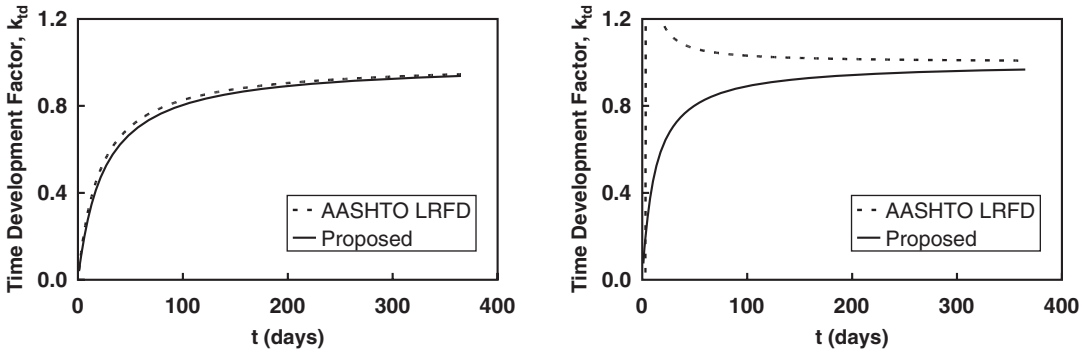

(a) k_{td} for f'_{ci} = 10 ksi (69 MPa) **(b)** k_{td} for f'_{ci} = 16 ksi (110 MPa)

Figure 2-8. Comparison of time-development correction factors.

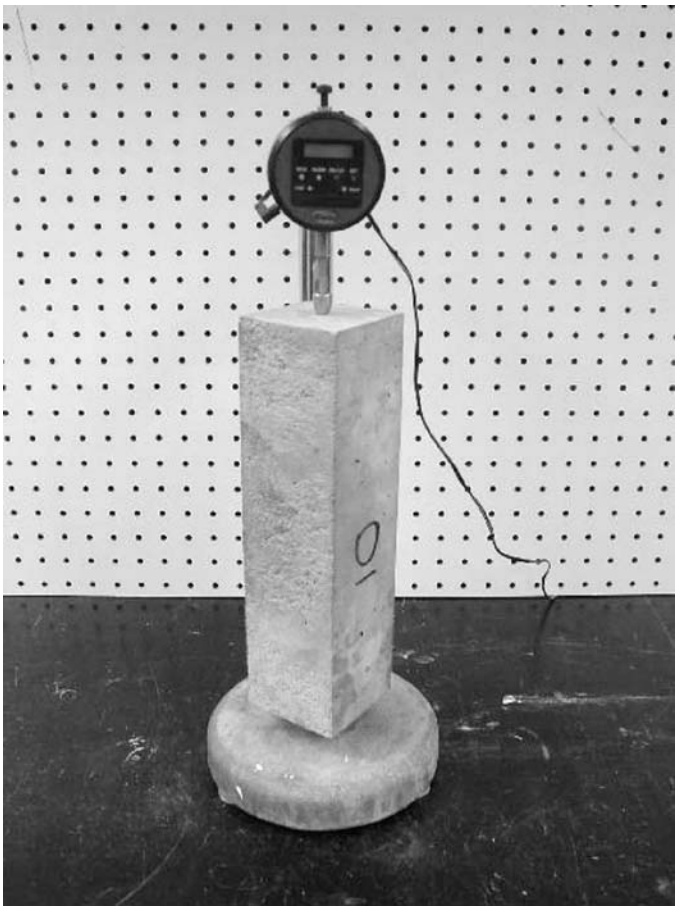

Figure 2-9. Test set-up for shrinkage.

maximum compressive strain at the opposite face. The main parameter considered in the test program was the concrete compressive strength which varied from 10.4 to 16 ksi (72 to 110 MPa). The test set-up and a typical failure mode of eccentric bracket test are shown in Figures 2-10 and 2-11. More detailed discussions are given in Appendix B.

The generalized stress distribution or the stress block in the compression zone of a flexural member can be defined by three parameters, k_1, k_2, and k_3, as shown in Figure 2-12. The parameter k_1 is the ratio of the average compressive stress to the maximum compressive stress, $k_3 f'_c$, in the compression zone. The parameter k_2 is the ratio of the depth of the resultant compressive force, C, to the depth of the compression zone, c. The parameter k_3 is the ratio of the maximum compressive stress in the compression zone to the compressive strength measured by concrete cylinder, f'_c. The design values of the stress block parameters are determined when the strain at the extreme fiber reaches the ultimate strain of the concrete, ϵ_{cu}. The three generalized parameters of the stress block can be reduced to two parameters to establish an equivalent rectangular stress block using α_1 and β_1, with the compressive stress resultant remaining at the same location. These parameters are also shown in Figure 2-13.

The test results from this research, as well as other researches reported in the literature, indicate that the generalized stress block parameter k_1 is seldom less than 0.58 for concrete compressive strengths varying from 10 to 18 ksi (69 to 124 MPa). Also, the stress distribution is almost linear for

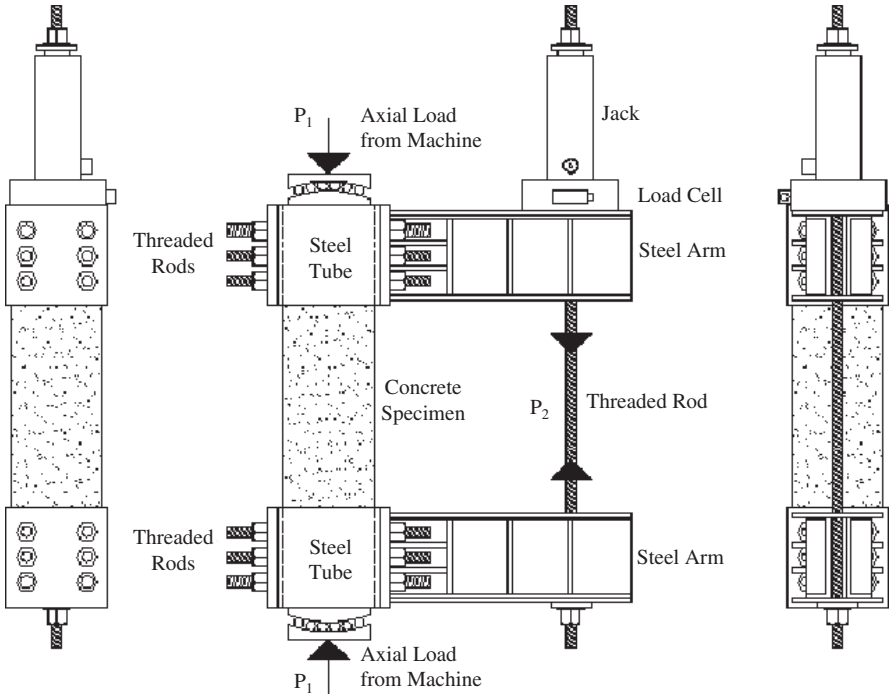

Neutral Face View

Figure 2-10. Test set-up of eccentric bracket specimens.

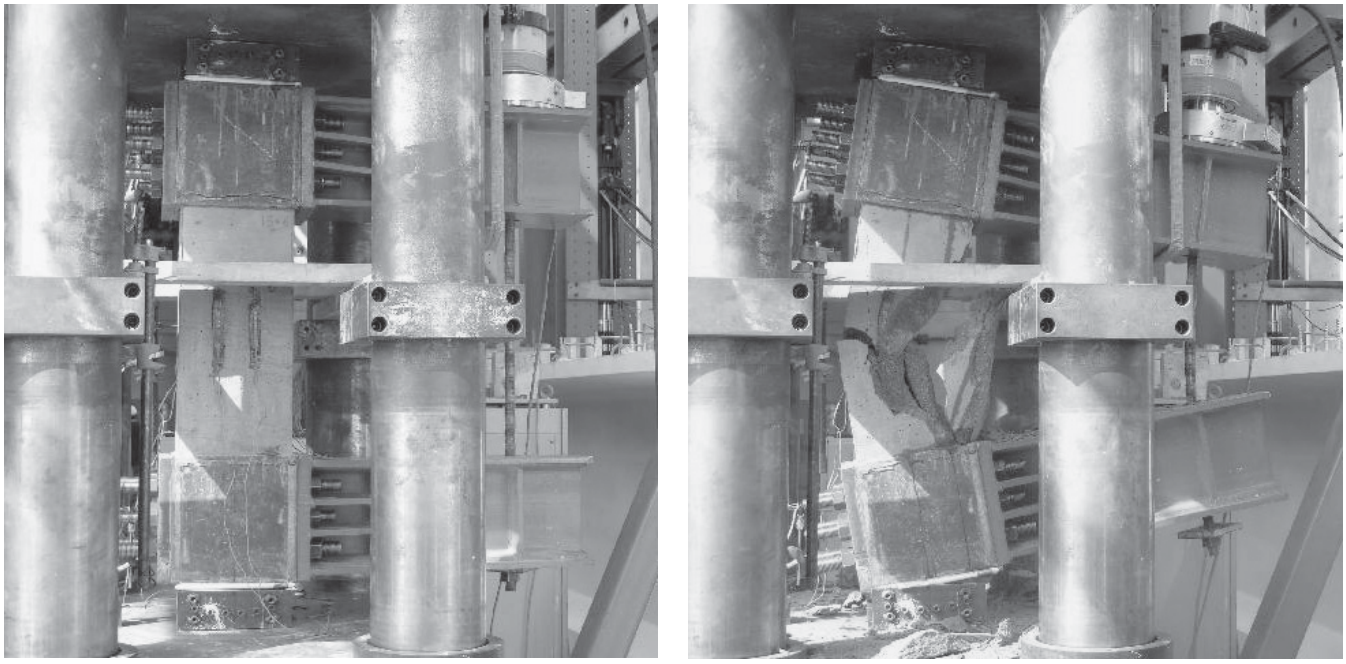

(a) Before testing **(b)** After testing

Figure 2-11. Typical failure mode for eccentric bracket specimens (18EB6).

HSC between 8 and 18 ksi (55 and 124 MPa) and, therefore, k_2 can be taken as 0.33. Furthermore, it was found that, for design purposes, it is suitable to use the same k_3 parameter, 0.85, for NSC as well as HSC with compressive strengths up to 18 ksi (124 MPa). Based on these observations, the following relationship is proposed for the rectangular stress block parameters, α_1 and β_1, for concrete compressive strengths up to 18 ksi (124 MPa).

$$\alpha_1 = \begin{cases} 0.85 & \text{for } f_c' \le 10 ksi \\ 0.85 - 0.02(f_c' - 10) \ge 0.75 & \text{for } f_c' > 10 ksi \end{cases} (f_c' \text{ in ksi})$$
$$\alpha_1 = \begin{cases} 0.85 & \text{for } f_c' \le 69 MPa \\ 0.85 - 0.003(f_c' - 69) \ge 0.75 & \text{for } f_c' > 69 MPa \end{cases} (f_c' \text{ in MPa}) \quad (2\text{-}4)$$

$$\beta_1 = \begin{cases} 0.85 & \text{for } f_c' \le 4 ksi \\ 0.85 - 0.05(f_c' - 4) \ge 0.65 & \text{for } f_c' > 4 ksi \end{cases} (f_c' \text{ in ksi})$$
$$\beta_1 = \begin{cases} 0.85 & \text{for } f_c' \le 28 MPa \\ 0.85 - 0.0073(f_c' - 28) \ge 0.65 & \text{for } f_c' > 28 MPa \end{cases} (f_c' \text{ in MPa}) \quad (2\text{-}5)$$

The comparisons of the above proposed relationships to the test results of this research and other data reported in the literature are shown in Figure 2-14 and Figure 2-15. The data for stress block parameters include test results obtained by Hognestad et al. (*22*), Nedderman (*23*), Kaar et al. (*24*, *25*), Swartz et al. (*17*), Pastor (*26*), Schade (*27*), Ibrahim (*28*), and Tan and Nguyen (*29*).

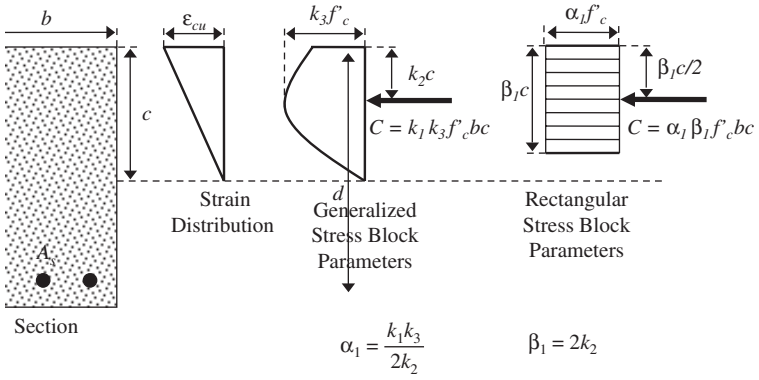

Figure 2-12. Stress block parameters for rectangular sections.

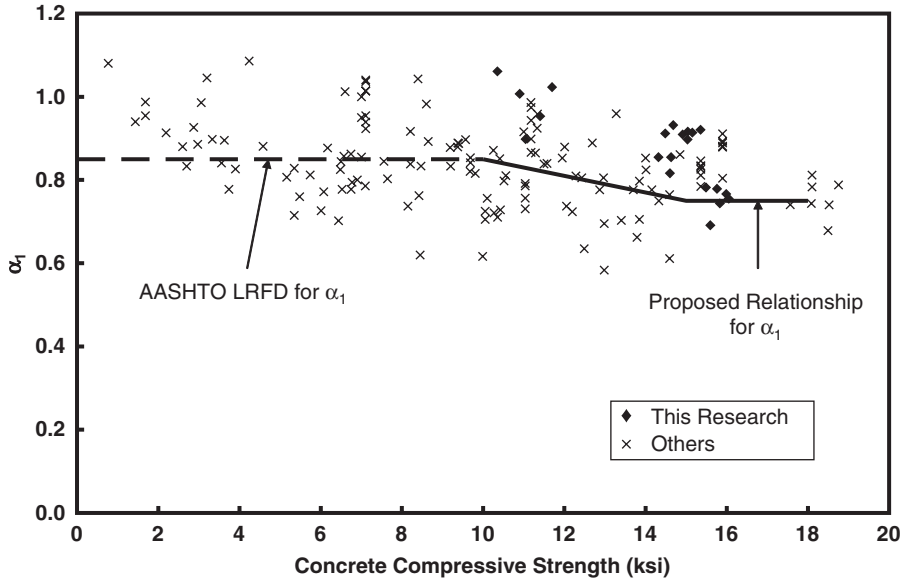

Figure 2-13. Proposed relationship for the rectangular stress block parameter α_1.

A sensitivity analysis was performed to evaluate how the ultimate flexural strength of a reinforced concrete member would be affected by the variations of the rectangular stress block parameter α_1. The results of the sensitivity analysis are shown in Figure 2-16, which indicate that for under-reinforced concrete section, the variations in the rectangular stress block parameters, α_1, have very small effect on the ultimate moment capacity of the section. On the other hand, for balanced and over-reinforced concrete sections, the same variations would affect the ultimate moment capacity of the sections significantly.

2.3.2 Flexural Behavior of HSC Beams

Fourteen reinforced HSC beams were tested under flexure with concrete strength, reinforcement ratio, specimen size, and specimen shape as main parameters. Typical failure of HSC beams is given in Figure 2-17. Detailed descriptions of those tests are given in Appendix C.

Shown in Figure 2-18 is a comparison of the measured ultimate moment, $M_{Exp,}$ with the predicted moment capacity, $M_{LRFD,}$ for all the beams tested in this study, as well as the data obtained from literature with concrete strengths over 10 ksi

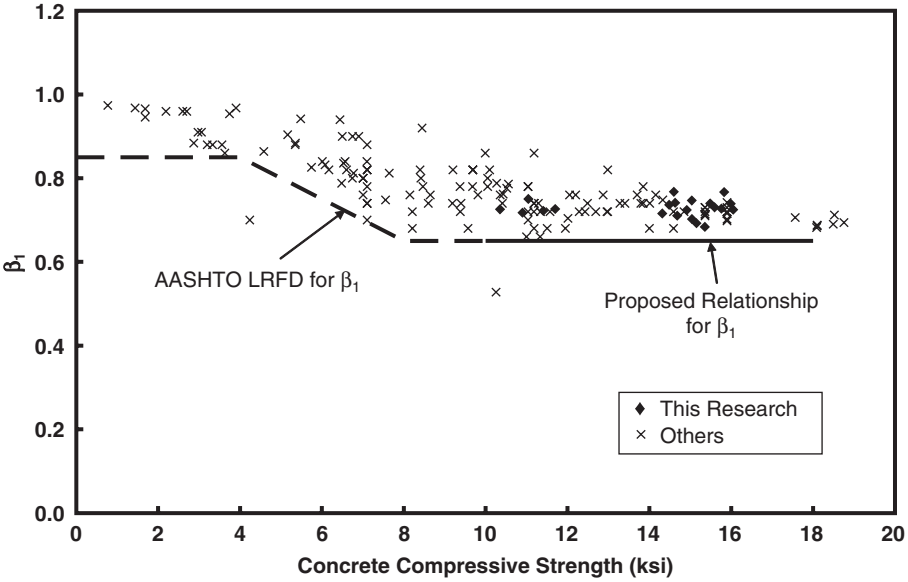

Figure 2-14. Proposed relationship for the rectangular stress block parameter β_1.

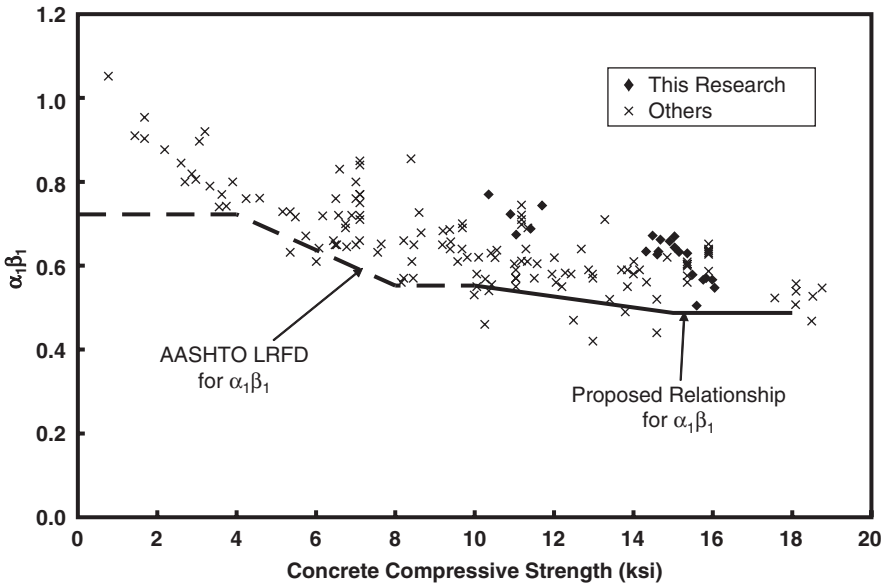

Figure 2-15. Proposed relationship for the product of rectangular stress block parameters $\alpha_1\beta_1$.

(69 MPa). For under-reinforced flexural specimens, the predicted moment capacity is based on the LRFD Specifications Equation 5.7.3.2.2.1, using the current value of 0.85 for α_1, 0.65 for β_1, and the measured material properties. For over-reinforced specimens or axial-flexural specimens, the moment capacity is determined by considering force equilibrium and strain compatibility. An ultimate strain value of 0.003 is assumed in the calculation, and plane sections are considered to remain plane.

The moment capacity is also determined by the proposed stress block parameters (see Appendix B), with a reduced value for α_1. The predicted moment capacity, M_{Prop}, is compared with the measured moment capacity, M_{Exp}, in Figure 2-19.

The results presented in Figures 2-18 and 2-19 indicate that using the proposed value of α_1 leads to a more conservative prediction of the nominal moment capacity for all the specimens tested in this project. Table 2-1 shows the statistical information of the predicted values of M_{LRFD} and M_{Prop} versus the measured values of M_{Exp} for a total of 141 specimens in the database (including those tested in the present study). The prediction using proposed α_1 value is slightly more conservative than using the existing α_1 value in the LRFD Specifications.

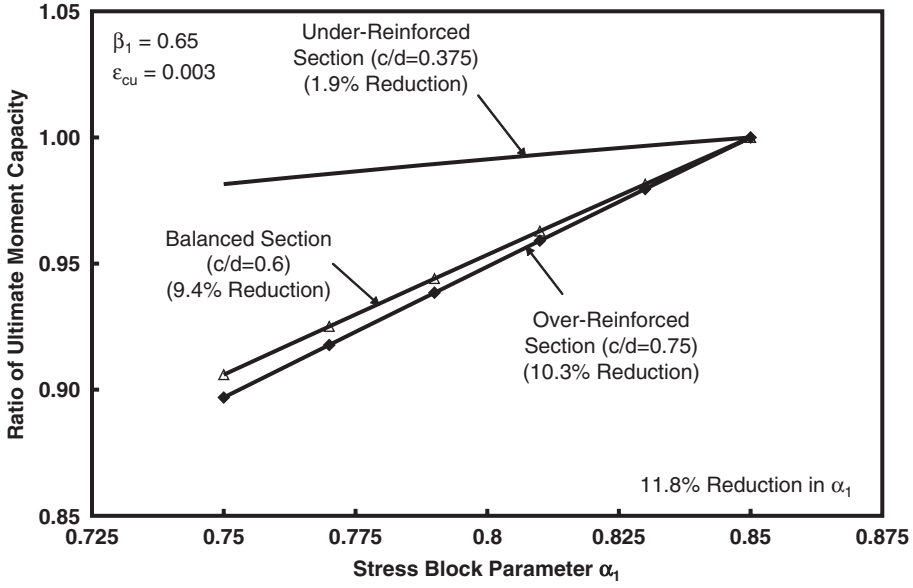

Figure 2-16. Ratio of ultimate moment capacity versus change in α_1 from 0.85 to 0.75.

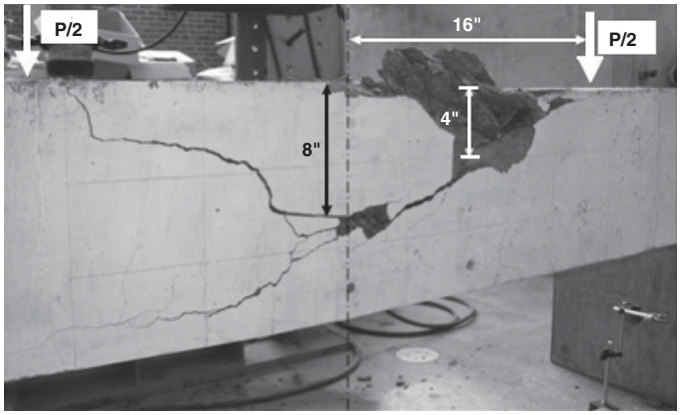

Figure 2-17. Typical failure of a pure flexure specimen (10B5.7).

2.3.3 Deflection

The mid-span deflections of the 13 beams tested in this project under 4-point bending are compared with the predicted values using the equations specified by the LRFD Specifications in Table 2-2. Three different elastic moduli were used in the calculations of deflections in Table 2-3 based on the new expression for the elastic modulus of HSC proposed in this study, the current equation according to the LRFD Specifications, and the measured elastic modulus. The moment of inertia of the cracked section I_{cr} is dependent on the elastic modulus of concrete, for the latter is used in establishing the transformed section. Therefore, I_{cr} needs to be re-calculated each time the elastic modulus of concrete is changed.

Table 2-2 indicates that the current LRFD Specifications under-estimates the deflection for all tested specimens in this project. The closest prediction is obtained by using the measured elastic modulus from cylinder tests. Using the proposed expression of the elastic modulus improves the prediction of deflection only slightly, when compared with the current equation specified by the LRFD Specifications.

Similar results have been reported in the literature as summarized by Rashid and Mansur (*30*) in Table 2-3, which is updated to include test results of this study for comparison.

Equation 5.7.3.6.2-1 of the current LRFD Specifications was proposed by Branson in 1963 based on test results of NSC members, and it was adopted by the ACI 318 (*2*) code in 1971. A statistical study of short-term deflection of simply supported beams was conducted by ACI Committee 435 in 1972. It was reported that, under controlled laboratory conditions, there is a 90-percent chance that deflection of a beam would fall within −20 to +30 percent of the calculated value. Therefore, a high degree of accuracy cannot be expected for deflection predictions.

The current LRFD Specifications tend to under-estimate the measured deflection for non-prestressed HSC beams. However, the discrepancy is within the commonly acknowledged limit for NSC. Because data on deflection of reinforced HSC beams is rather limited, it is not justified to propose any changes to the current equations specified by the LRFD Specifications (*1*) for deflection calculation.

2.3.4 Cracking

The observed and predicted cracking loads are summarized in Table C4 (Appendix C). Generally speaking, the observed and the predicted values are not in good agreement. This discrepancy can be attributed to inaccuracies from both

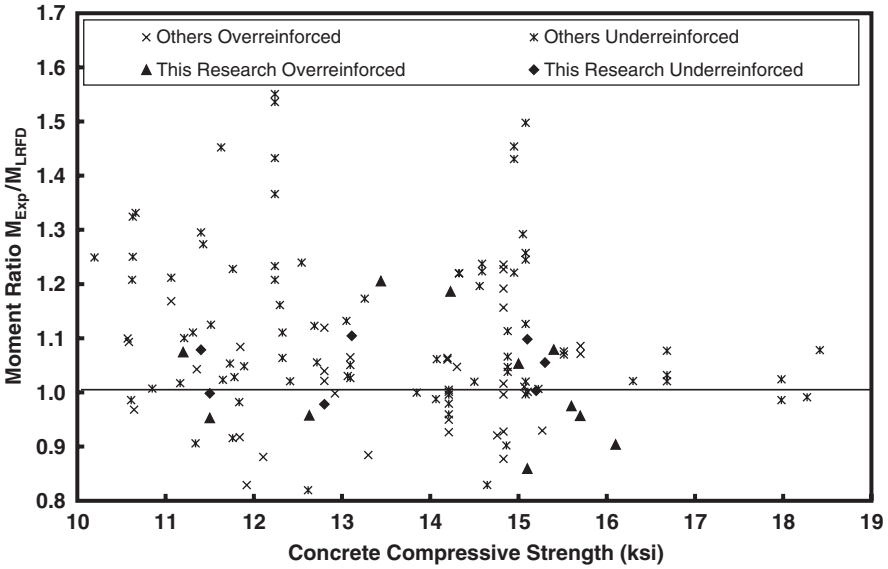

Figure 2-18. Comparison of the experimental and predicted values of flexural resistance using the current LRFD Specifications (1).

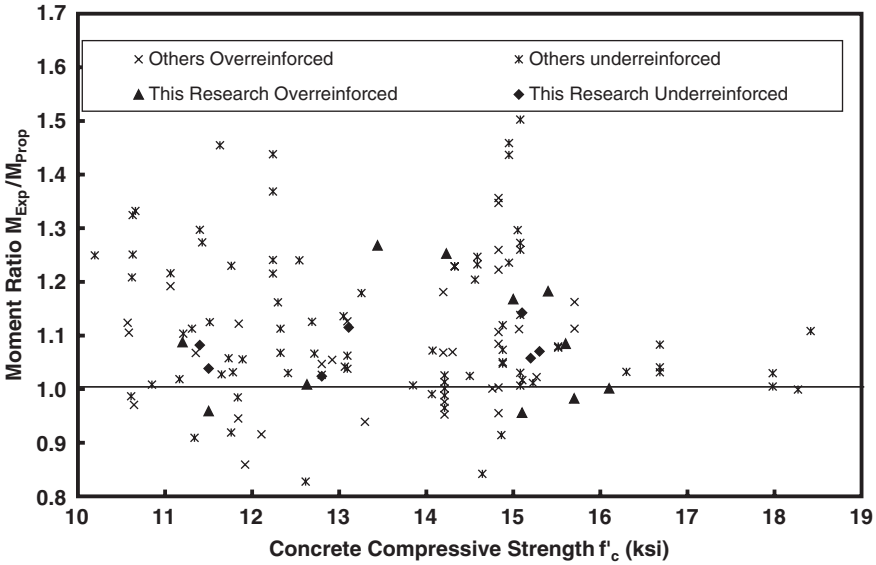

Figure 2-19. Comparison of the experimental and predicted values of flexural resistance using the proposed stress block factors.

the observed and the predicted data. The inaccuracy of the observed data is likely from the following two sources:

1. The first cracking could not be recognized until it propagated to the side surface of the specimen, and the very fine cracks could not be detected readily. Therefore, it is believed that the reported value is usually slightly over-estimated.
2. The cracking load obtained from the load-deflection curve is only an estimate. The development of micro-cracks is gradual and the reduction of member stiffness occurs slowly. As a result, the change in the slope of the load-deflection curve is not sudden and distinctive.

2.3.5 Crack Width

Crack width was measured using pi-gages installed on the bottom surface of the specimens. Readings were adjusted based on the neutral axis depth to reflect the crack width at the extreme tension fiber of the specimen. The reported values are the readings at 45 percent of the measured peak load, which is considered to represent the average level of the service load.

The measured crack widths for the tested flexure members are shown in Figure 2-20. The crack width of 0.017 in. (0.425 mm), as specified for Class 1 exposure condition, is also shown in the same figure. As expected, given that all the specimens tested in this project used mild steel reinforcement with spacings not exceeding the allowable value specified by Equation 5.7.3.4.1 of the LRFD Specifications, all of the measured crack widths are less than 0.017 in. (0.425 mm).

The current equation for crack control specified by the LRFD Specifications is based on a physical crack model developed by Frosch (*37*), rather than the statistically based model used in previous editions of the specifications. In Figure 2-21, measured crack widths are compared with the predicted values using Frosch's model. In calculating the crack width, the actual measured steel strains were used. Frosch's model over-estimates the crack width for most of the beams tested in this project. Only six over-reinforced beams, in which the steel stress at service load was much lower than $0.6 f_y$, developed crack widths that are under-estimated by the Frosch model.

2.3.6 Ultimate Concrete Strain

The ultimate compressive strain of concrete measured from eccentric bracket specimens, eccentrically loaded columns, beams tested under flexure, beams tested under combined

Table 2-1. Statistical data for over-reinforced and under-reinforced HSC beams.

Type	Total Number of Specimens	M_{Exp}/M_{LRFD}					M_{Exp}/M_{prop}				
		<1	Min	Max	Avg.	Std. Dev.	<1	Min	Max	Avg.	Std. Dev.
Over-Reinf.	52	19	0.83	1.59	1.07	0.15	12	0.86	1.59	1.11	0.14
Under-Reinf.	91	16	0.82	1.55	1.12	0.15	11	0.83	1.55	1.13	0.15

Table 2.-2. Comparison of measured and predicted mid-span deflections at service load for the pure flexure specimens.

Specimen No.	$\frac{\Delta_{Measured}}{\Delta_{Predicted}}$ using E from		
	LRFD	Proposed	Measured
10B2.1	1.19	1.18	1.10
10B4.3	1.23	1.20	1.11
10B5.7	1.12	1.10	1.02
10B10.2	1.33	1.32	1.08
14B3.3	1.30	1.28	1.22
14B7.7	1.23	1.23	1.14
14B12.4	1.27	1.25	1.14
14B7.6	1.23	1.20	1.14
14B12.7	1.33	1.28	1.22
14B17.7	1.30	1.25	1.18
18B5.9	1.45	1.41	1.19
18B12.7	1.52	1.47	1.20
18B17.7	1.28	1.25	1.01
Average	1.29	1.26	1.13
Std. Dev.	0.103	0.096	0.070

axial and flexural loading, and prestressed beams as fully described in the appendixes are shown in Figure 2-22. This figure shows the measured values from this research as well as the data obtained from literature (except for the cases of eccentrically loaded columns and prestressed concrete girders). Based on these test results, the currently specified compressive strain limit of 0.003 is considered applicable for the full range of concrete compressive strengths up to 18 ksi (124 MPa).

2.4 Compression Members

This section summarizes the research findings from the tests performed to evaluate the behavior of HSC compression members. The findings include information on axial resistance, longitudinal, and transverse reinforcement requirements. The experimental program consisted of columns subjected to concentric and eccentric loadings as well as flexural members subjected to axial compression load. Details of these studies are provided in Appendixes C and D.

2.4.1 Axial Resistance

A total of 32 rectangular and 24 circular columns with concrete strengths ranging from 7.9 to 16.5 ksi (54 to 114 MPa) were tested under monotonically increasing concentric and eccentric loading. The test parameters for concentric loading included concrete strength, specimen size and shape, longitudinal reinforcement ratio, and amount of transverse reinforcement. For eccentric loading, concrete strength, specimen size, and eccentricity of the applied load were the test parameters.

Test results from this study were compiled with reported data in the literature to examine the validity of the current specifications for HSC up to 18 ksi (124 MPa). Studies were performed mainly for the load carrying capacity of short columns with concrete compressive strength greater than 10 ksi (69 MPa), subjected to axial loading and combined axial and flexural loading, and for the behavior of the columns with tie and spiral steel as transverse reinforcement.

Figure 2-23 shows different failure modes of a rectangular column with tie reinforcement and a circular column with spiral reinforcement under concentric loading.

The general behavior of reinforced concrete columns can be characterized sequentially by the initiation of surface cracks, spalling of cover concrete, yielding of longitudinal steel, buckling of longitudinal reinforcement, crushing of core concrete, yielding of transverse reinforcement, and, finally, fracture of transverse reinforcement. However, the behavior of each individual column was highly dependent on the amount of transverse reinforcement. In the rectangular columns with ties spaced according to the LRFD Specifications, yielding and fracture of transverse reinforcement did not occur even at later stage of loading.

The nominal axial load carrying capacity of a column at zero eccentricity, P_o, can be determined by using the force equilibrium equation:

$$P_o = k_c f_c' (A_g - A_s) + f_y A_s \qquad (2\text{-}6)$$

Table 2-3. Statistical information on service load deflection from literature.

Researchers	No. of Beams	f'_c (ksi)	ρ (%)	$\frac{\Delta_{Measured}}{\Delta_{Predicted}}$	
				Average	σ
Rashid and Mansur a (*30*)	16	6.2 – 18.3	1.3 – 5.3	1.26	0.08
Ashour (*31*)	9	7.1 – 14.8	1.2 – 2.4	1.17	0.07
Lin (*32*)	9	3.9 – 10	2 – 3.7	1.27	0.12
Lambotte and Taerwe (*33*)	5	4.9 – 11.7	0.5 – 1.5	1.17	0.12
Paulson et al. (*34*)	9	5.4 – 13.2	1.5	1.37	0.14
Shin et al. (*35*)	23	3.9 – 14.5	0.4 – 3.6	1.56	0.27
Pastor et al. (*36*)	12	3.8 – 9.3	1.1 – 5.3	1.09	0.08
This Research	13	11.4-16.1	2.1-17.7	1.29	0.10

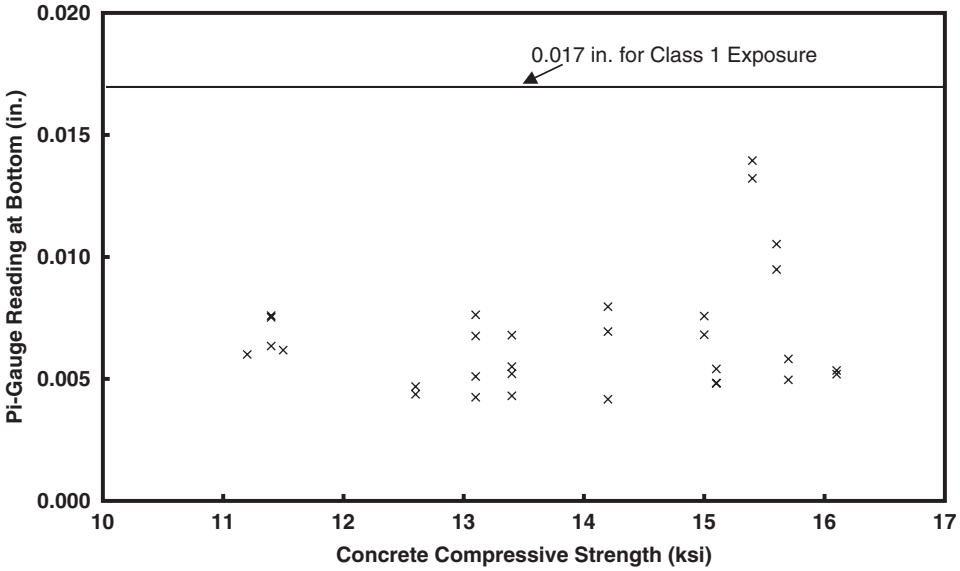

Figure 2-20. Measured crack width vs. concrete strength at service load.

where the parameter k_c is the ratio of the in-place concrete strength to the compressive strength of control cylinder, f'_c, A_g is the gross area of the column, f_y is the yield strength of longitudinal reinforcement, and A_s is the area of longitudinal reinforcement.

The parameter k_c accounts for the size effect, shape, and concrete casting process of column versus standard concrete cylinder. The current value for k_c specified by the LRFD Specifications for a concentrically loaded column is 0.85 for NSC.

Figure 2-24 shows the value for k_c based on the test results of concentrically loaded columns with ties obtained in this study along with the test data found in the literature by Tan and Nguyen (*29*), Cusson and Paultre (*38*), Sheikh and Uzumeri (*39*), Saatcioglu and Ravzi (*40*), Sharma et al. (*41*), Yong et al. (*42*), and Nagashima et al. (*43*). The data shown in this figure also include columns with closer tie spacing than that required by the LRFD Specifications.

The data in the figure clearly show a trend that the parameter k_c obtained from the concentrically loaded rectangular columns, tested in this project, decreases with increasing concrete strength for concrete strength higher than 10 ksi (69 MPa). A regression analysis of the collected data, shown in Figure 2-24, indicates that 80 percent of the k_c values are higher than 0.75 for concrete strength greater than 10 ksi

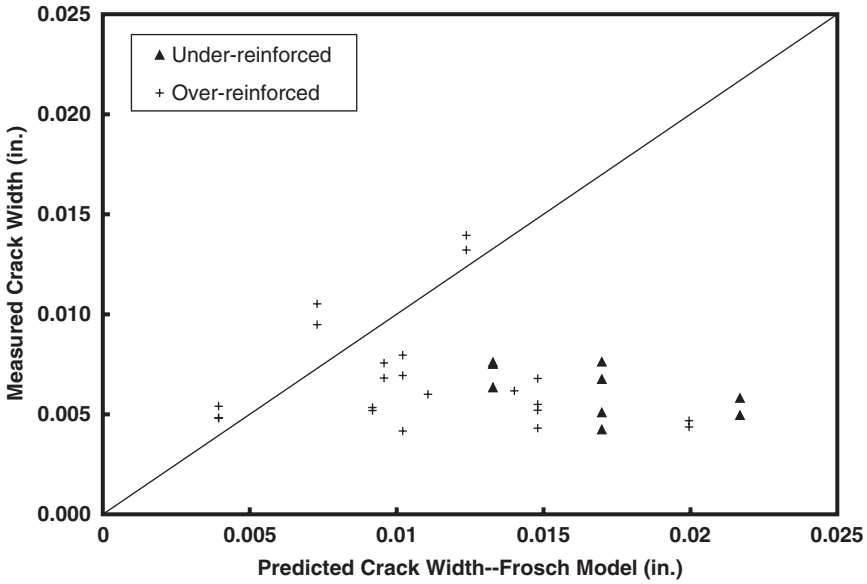

Figure 2-21. Measured vs. predicted crack width using Frosch's model (37) at service load.

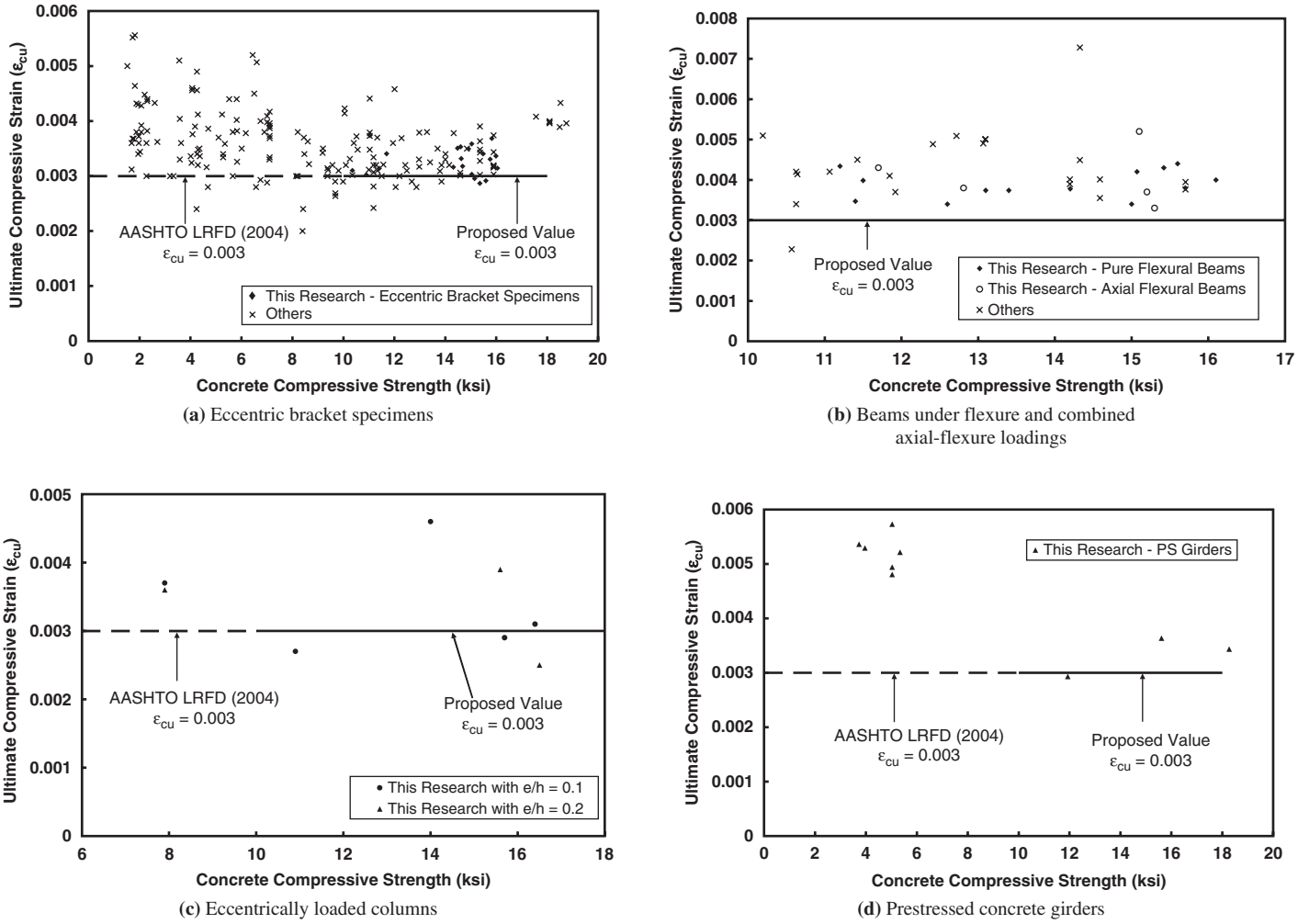

(a) Eccentric bracket specimens

(b) Beams under flexure and combined axial-flexure loadings

(c) Eccentrically loaded columns

(d) Prestressed concrete girders

Figure 2-22. Measured ultimate compressive strain of concrete.

(69 MPa). Based on the above observations, the following expression for the parameter k_c is proposed as a revision for the LRFD Specifications.

$$k_c = \begin{cases} 0.85 & for\ f_c' \le 10ksi \\ 0.85 - 0.02(f_c' - 10) \ge 0.75 & for\ f_c' > 10ksi \end{cases} (f_c' \text{ in ksi}) \quad (2\text{-}7)$$

$$k_c = \begin{cases} 0.85 & for\ f_c' \le 69MPa \\ 0.85 - 0.003(f_c' - 69) \ge 0.75 & for\ f_c' > 69MPa \end{cases} (f_c' \text{ in MPa})$$

The proposed expression maintains the current value of k_c as specified by the LRFD Specifications for NSC and extends its value for HSC up to 18 ksi (124 MPa).

For circular columns with spiral reinforcement, the measured load corresponding to the initial spalling of concrete cover, P_{CR}, was used to determine the parameter k_c for circular columns using the equation of P_o. The k_c parameters obtained from the concentrically loaded circular columns, tested in this project, as well as other reported tests by Sharma et al. (*41*), Issa and Tobaa (*44*), and Liu et al. (*45*) are shown in Figure 2-25. The same trend of k_c for the rectangular columns could be observed for the circular columns.

Although the load carried by the circular column corresponding to the initiation of concrete spalling was used to determine the value of k_c, the capacity of the circular columns would continue to increase after the spalling of the concrete cover because of the confinement effect produced by the spiral reinforcement. Accordingly, the expression for k_c proposed for columns with ties can be used safely for the columns with spiral reinforcement.

2.4.2 Longitudinal Reinforcement Limits

The upper reinforcement limits for compression members were initially established based on practical considerations of concrete placement and have since been maintained for all ranges of concrete compressive strengths. Therefore, the relationships specified by the LRFD Specifications are applicable for concrete compressive strengths up to 18 ksi (124 MPa).

The current LRFD Specifications require extremely high levels of minimum reinforcement ratio for compression members for concrete compressive strengths over 10 ksi (69

(a) Rectangular column with tie reinforcement

(b) Circular column with spiral reinforcement

Figure 2-23. Failure shapes of tested columns under concentric loading.

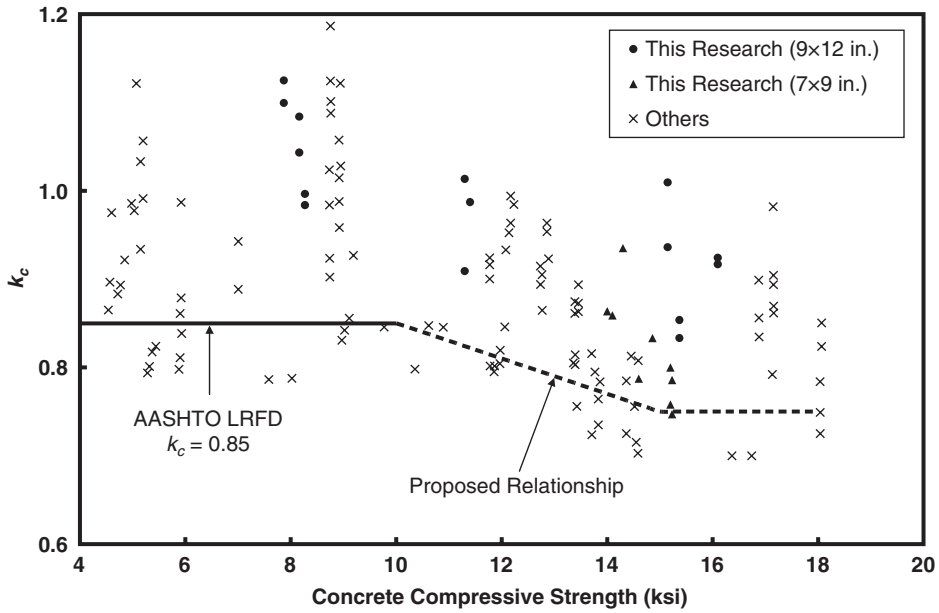

Figure 2-24. Comparison of parameters k_c of concentrically loaded columns with ties.

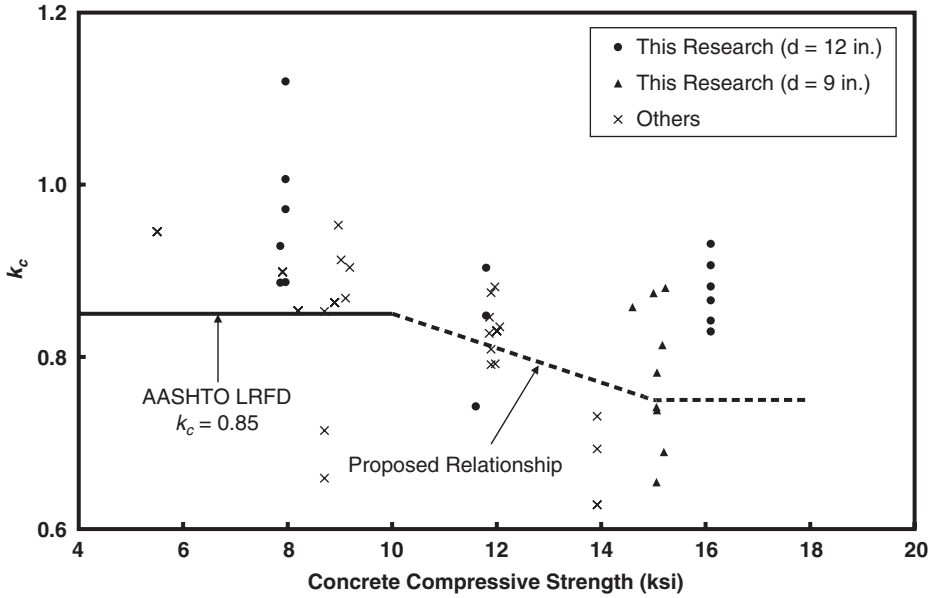

Figure 2-25. Comparison of k_c parameters of concentrically loaded columns with spiral reinforcement.

MPa). Based on the performed analysis using the proposed equation for E_c and the current relationship specified by the LRFD Specifications presented in Appendix D, a new relationship is proposed for minimum reinforcement ratio for compression members as follows:

$$\frac{A_s}{A_g}+\frac{A_{ps}f_{pu}}{A_g f_y}\geq 0.135\frac{f_c'}{f_y} \text{ but not greater than } 0.0225. \qquad (2\text{-}8)$$

where f_c' is the concrete compressive strength, A_{ps} is the area of prestressing steel, f_{pu} is the specified tensile strength of prestressing steel, A_s and f_y are the area and yield strength of mild tension steel, respectively, and A_g is the gross area of the section.

Figure 2-26 shows the comparison, for the stress level $P/f_c' A_g = 0.5$, among the minimum longitudinal reinforcement ratio required by the current LRFD Specifications, the above proposed revision, and the theoretical requirement by considering concrete rupture due to the effects of creep and shrinkage as explained in Appendix D. The figure clearly indicates that for concrete strength greater than 10 ksi (69 MPa), the required minimum longitudinal reinforcement ratio by the proposed equation is greatly reduced from that called for by the current LRFD Specifications, but the

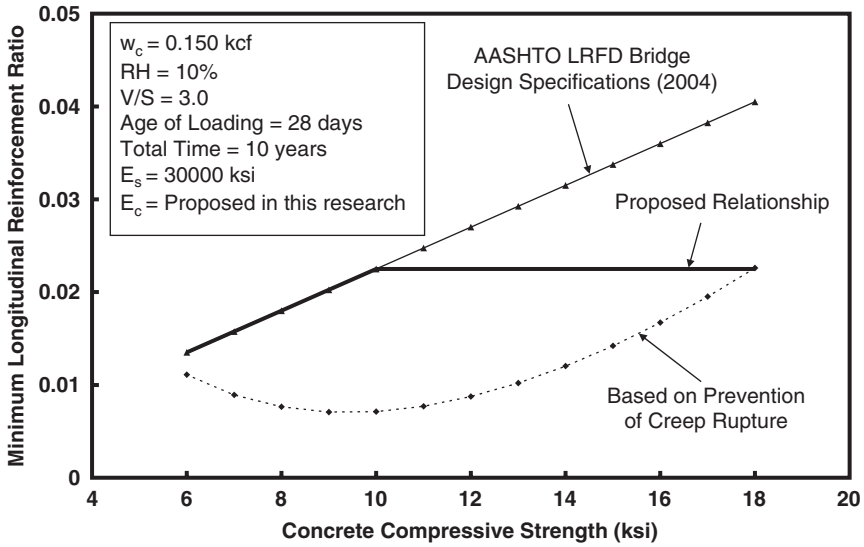

Figure 2-26. Comparison of the A_s/A_g ratio for $P/f_c' A_g = 0.5$.

proposed equation still provides substantial margin against what is needed to prevent creep rupture.

2.4.3 Transverse Reinforcement

2.4.3.1 Rectangular Columns with Tie Reinforcement

In this test program, the spacing of ties in rectangular columns was designed by two criteria, one according to the maximum spacing permitted by the LRFD Specifications, and the other as half of what is permitted by the LRFD Specifications. The measured strains in the longitudinal reinforcement exceeded the yield strain at the peak load, which occurred in all tested columns with tie reinforcement. The measured strains in the ties of the columns with larger tie spacing were considerably lower than the yield strain of the ties. These results suggest that ties in the columns spaced according to what is allowed by the LRFD Specifications are sufficient to provide adequate lateral support for preventing buckling of longitudinal reinforcement below the yield strength. However, the tested columns with such large tie spacing did not show any confinement effect to the concrete core as confirmed also by other researchers. Based on the results, there is no need to modify the current provisions for the tie requirement specified by the LRFD Specifications for HSC.

2.4.3.2 Circular Columns with Spiral Reinforcement

In reinforced concrete columns with an effectively confined core (usually columns with spiral reinforcement), the confinement effect produced by transverse reinforcement can greatly improve the strength and ductility of the columns. A minimum volumetric ratio of spiral, ρ_s is required by the LRFD Specifications to ensure that the second maximum load carried by the column core and longitudinal reinforcement would roughly equal the initial maximum load carried by the column before spalling of the concrete cover. Based on test results from this project, the second peak loads are generally larger than the first peak loads in most columns with volumetric ratio of spiral close to the code requirement, which is a favorable behavior satisfying the premise of the code. Accordingly, it can be concluded that the current minimum spiral steel requirement of the LRFD Specifications is also applicable to HSC columns.

2.4.4 Resistance to Combined Axial and Flexural Loading

The behavior of members subjected to combined axial compression and flexure was investigated using two different types of specimens: (1) four beams tested under a constant axial load as shown in Figure 2-27 and (2) eight columns tested under small eccentricity as shown in Figure 2-28.

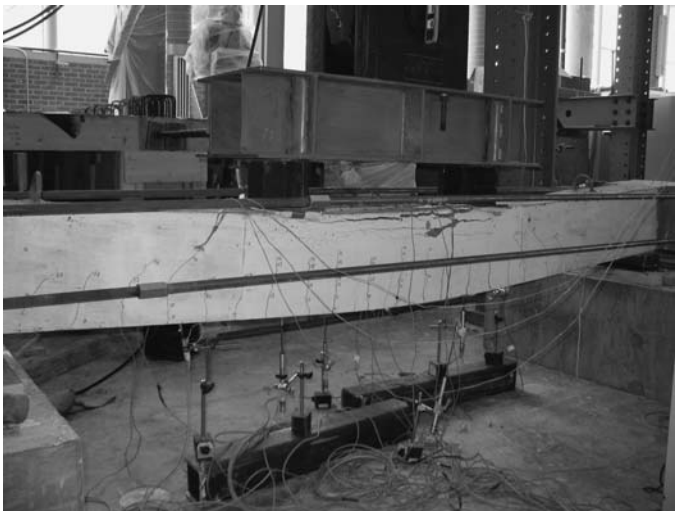

Figure 2-27. Beam tested under combined flexural and axial loading (10BA4).

The measured ultimate strengths of the tested columns and beams in this research are plotted with the interaction diagrams constructed using the current LRFD Specifications and with the proposed parameters α_1, β_1, and k_c as shown in Figure 2-29.

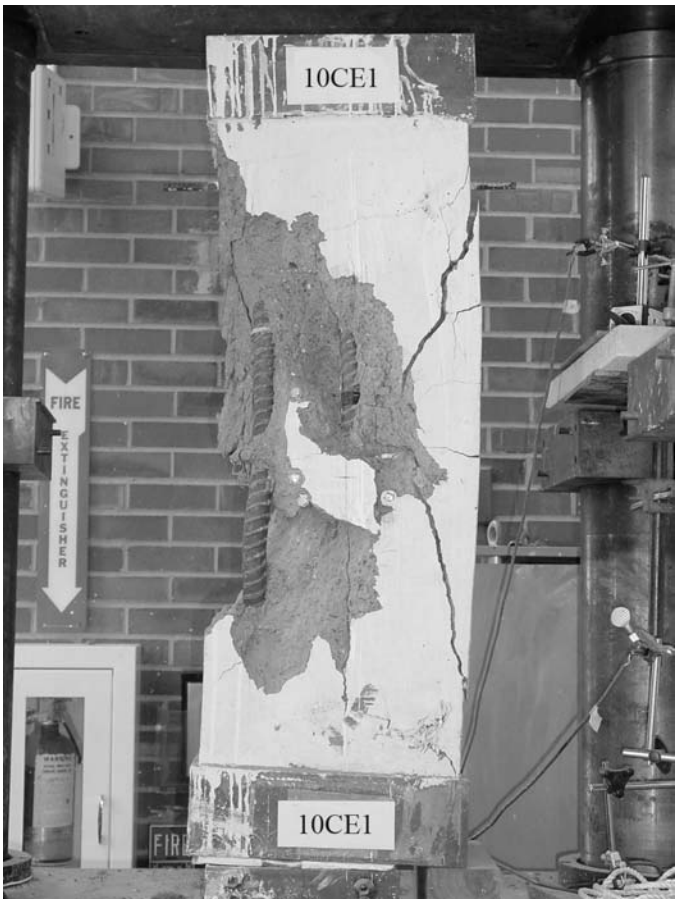

Figure 2-28. Rectangular column tested under small eccentricity (10CE1).

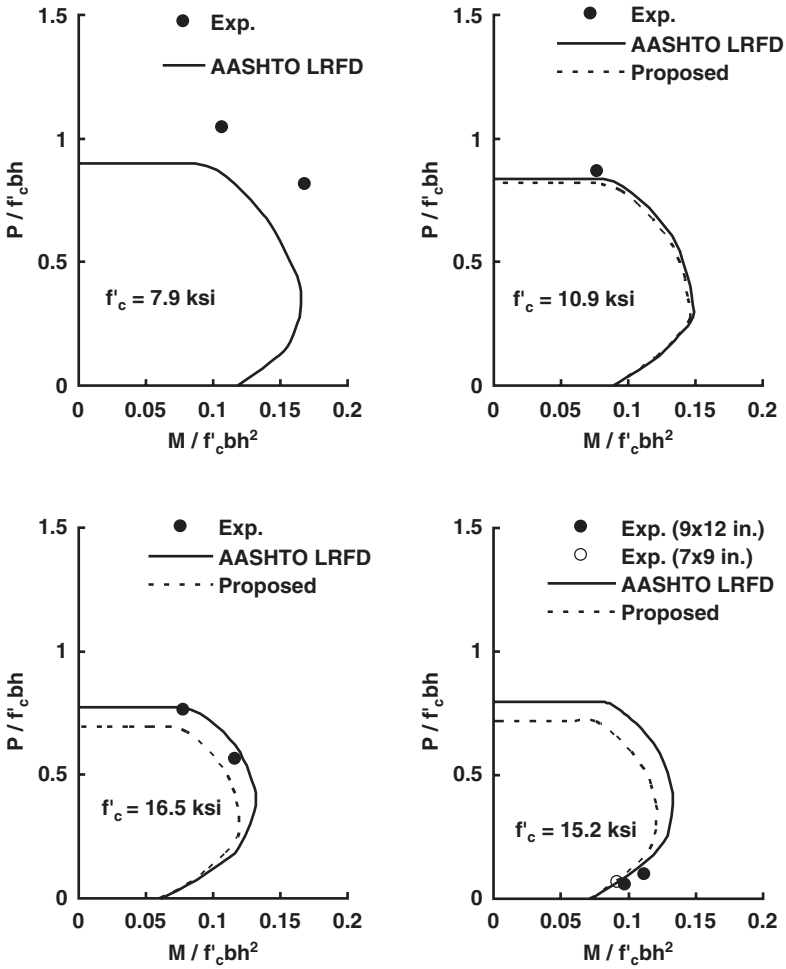

Figure 2-29. Interaction diagrams using LRFD Specifications (1) and the proposed parameters α_1, β_1, and k_c for each batch of concrete.

For concrete compressive strengths exceeding 10 ksi (69 MPa), the modified interaction diagrams according to the proposed parameters α_1, β_1, and k_c are more conservative than those based on the LRFD Specifications, especially for compression members subjected to small eccentricity as indicated by the test data.

2.5 Prestressed Concrete

Nine Type II prestressed concrete girders were tested to evaluate the applicability of the LRFD Specifications for the flexural response of prestressed HSC girders up to 18 ksi (124 MPa). The study also included an examination of the provisions for prestress loss and transfer length of prestressing strands in such girders.

The girders were produced in a prestressed concrete plant using three different target concrete compressive strengths: 10, 14, and 18 ksi (69, 97, and 124 MPa). Three identical girders were produced for each target concrete strength. Composite decks were subsequently cast on two of the three girders in each group, one of 5 ft. (1.5 m) width and the other of 1 ft. (0.3 m) width. The design concrete strength for the deck was 4 ksi (28 MPa). The third girder in each group was tested without a deck slab. Typical failure modes for the three groups of girders are shown in Figure 2-30. Detailed discussion of this experimental program for prestressed concrete girder is presented in the Appendix E.

2.5.1 Prestress Losses

The measured prestress losses for all the tested prestressed concrete beams are given in Table 2-4. The total loss of prestress for each of the nine test specimens were computed according to the LRFD Specifications. The computed prestress losses, including elastic shortening, creep, shrinkage, and relaxation, were compared with the prestress losses

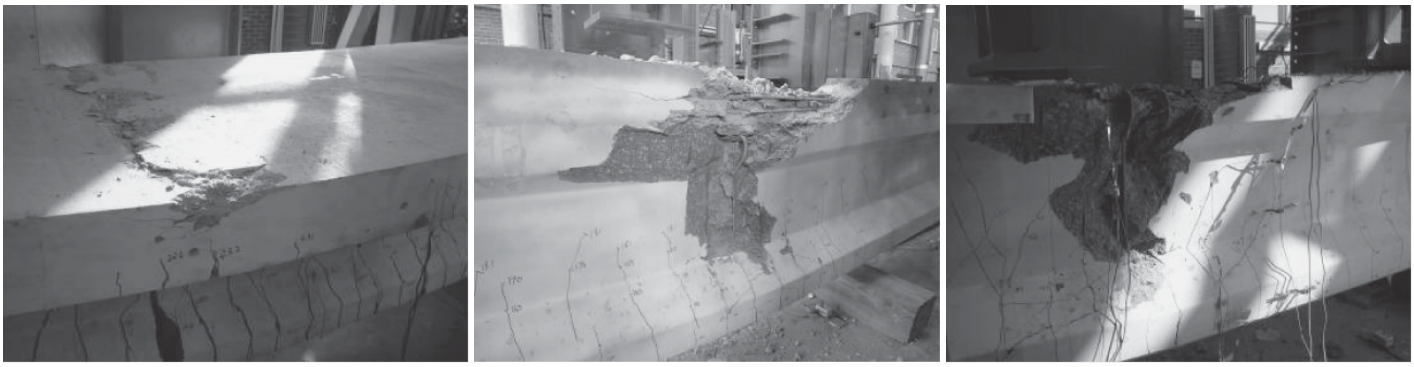

(a) Girder with a 5-ft. deck **(b)** Girder with a 1-ft. deck **(c)** Girder without a deck

Figure 2-30. Typical failure mode.

determined from the effective prestressing force based on the measured cracking moment and modulus of rupture. The comparisons indicate that the predicted prestress losses by using the provisions of the LRFD Specifications were comparable to the measured losses.

2.5.2 Flexural Resistance

The equation for calculating the cracking moment in the LRFD Specifications is highly dependent on the value of modulus of rupture and effective prestress. The cracking moments predicted by using the modulus of rupture specified in the LRFD Specifications and by the proposed equation for modulus of rupture (see Appendix A) are compared with the measured cracking moments in Figure 2-31.

The results indicate that the predicted cracking moment based on the modulus of rupture specified by the LRFD Specifications overestimated the measured cracking moment for seven of the nine tested girders. However, for all the tested girders, the predicted cracking moment using the proposed modulus of rupture produced conservative results. Given that the prestressed losses predicted by the LRFD Specifications are conservative as shown in Table 2.4, the unconservative prediction of the cracking moment is mainly due to the unconservative values used for modulus of rupture. Therefore, the proposed modulus of rupture, $f_r = 0.19\sqrt{f_c'(ksi)}$ ($f_r = 0.5\sqrt{f_c'(MPa)}$), is more appropriate for use in determining the cracking moment of prestressed HSC girders.

The flexural resistance, $M_{predicted}$, of each of the nine tested girders was computed (see Appendix E) and is compared with the measured flexural resistance, $M_{measured}$, in Figure 2-32. The comparison shows that the predicted flexural resistance was fairly conservative in all cases.

2.5.3 Transfer Length

Transfer length of all tested prestressed concrete beams was determined based on the measured end slippages of

Table 2-4. Summary of prestress losses.

Identification	Actual Prestress Losses (Using measured M_{cr} and f_r) (%)	Computed Total Prestress Losses	
		LRFD Eqn. (%)	Proposed Eqn. (%)
10PS-5S	12.9	13.9	13.7
14PS-5S	11.2	15.3	15.0
18PS-5S	12.9	14.2	14.2
10PS-1S	13.9	15.1	14.8
14PS-1S	10.8	15.8	15.6
18PS-1S	11.3	15.0	15.1
10PS-N	8.3	14.9	14.7
14PS-N	7.3	17.6	17.2
18PS-N	10.1	14.1	14.3
Average	**11.0**	**15.1**	**14.9**
Standard Dev.	**0.022**	**0.01**	**0.01**

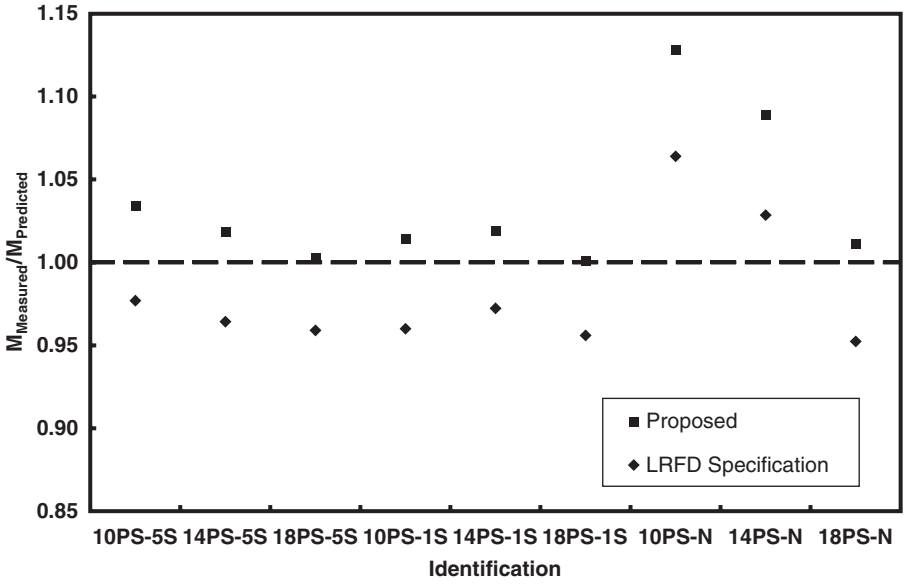

Figure 2-31. Cracking strength ratio of the measured versus predicted results.

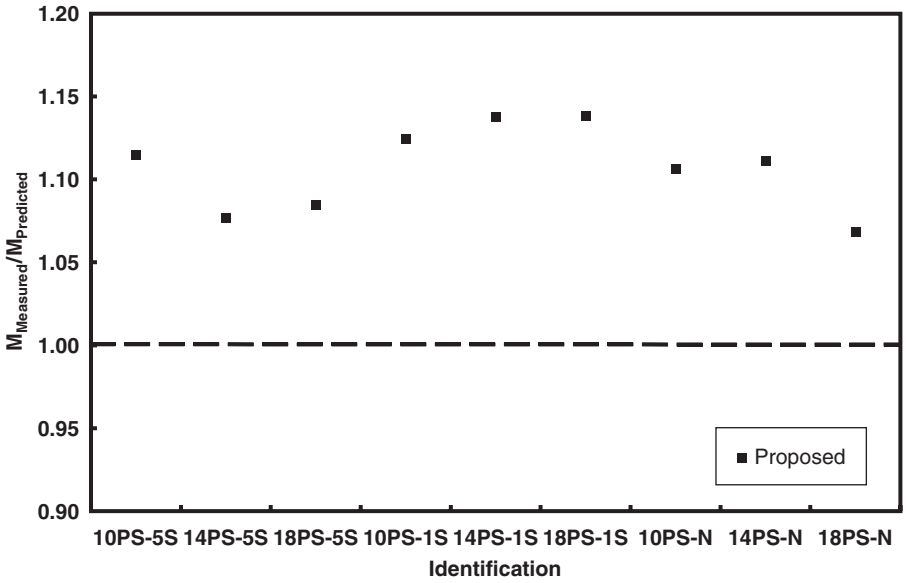

Figure 2-32. Flexural strength ratio of the measured versus predicted results.

strands at transfer. Test results indicate that the current provision of the LRFD Specifications provides appropriate prediction for the transfer length. Based on the data, LRFD Specifications may be used to determine transfer length of prestressed HSC girders with concrete compressive strength up to 18 ksi (124 MPa). Extensive research related to transfer length of prestressed HSC girder is in progress under NCHRP Project 12-60, "Transfer, Development, and Splice Length for Strand/Reinforcement in High-Strength Concrete."

CHAPTER 3

Proposed Revisions to AASHTO LRFD Bridge Design Specifications

Based on the research findings presented in Chapter 2 and details given in the appendixes, the following revisions are recommended in order to extend the applicability of the LRFD Specifications to include HSC up to compressive strengths of 18 ksi (124 MPa):

1. The current equation for time-development factor (k_{td}) (Equation 5.4.2.3.2-5 and Equation 3-1) in the LRFD Specifications relative to creep and shrinkage should be replaced by Equation 3-2.

$$k_{td} = \frac{t}{(61 - 4f_{ci}' + t)} \quad (f_{ci}' \text{ in ksi})$$
$$k_{td} = \frac{t}{(61 - 0.58f_{ci}' + t)} \quad (f_{ci}' \text{ in MPa}) \tag{3-1}$$

$$k_{td} = \frac{t}{12\left(\frac{100 - 4f_{ci}'}{f_{ci}' + 20}\right) + t} \quad (f_{ci}' \text{ in ksi})$$
$$k_{td} = \frac{t}{12\left(\frac{100 - 0.58f_{ci}'}{0.145f_{ci}' + 20}\right) + t} \quad (f_{ci}' \text{ in MPa}) \tag{3-2}$$

   where t is the age of concrete after loading in days, f_{ci}' is the specified compressive strength at prestress transfer for prestressed members or 80 percent of the strength at service for non-prestressed members.
2. The current equation for modulus of elasticity (E_c) (Equation 5.4.2.4-1 and Equation 3-3) in the LRFD Specifications should be replaced by Equation 3-4:

$$E_c(ksi) = 33000K_1\left(w_c(kcf)\right)^{1.5} \cdot \left(f_c'(ksi)\right)^{0.5}$$
$$E_c(MPa) = 0.043K_1\left(w_c(kg/m^3)\right)^{1.5} \cdot \left(f_c'(MPa)\right)^{0.5} \tag{3-3}$$

$$E_c(ksi) = 310000K_1\left(w_c(kcf)\right)^{2.5} \cdot \left(f_c'(ksi)\right)^{0.33}$$
$$E_c(MPa) = 0.000035K_1\left(w_c(kg/m^3)\right)^{2.5} \cdot \left(f_c'(MPa)\right)^{0.33} \tag{3-4}$$

   where K_1 is the correction factor for source of aggregate to be taken as 1.0, unless determined by physical test, and as approved by the authority of jurisdiction, w_c is the unit weight of concrete, and f_c' is the specified compressive strength of concrete.
3. The modulus of rupture (f_r) (Section 5.4.2.6) in the LRFD Specifications $0.24\sqrt{f_c'(ksi)}$ $(0.62\sqrt{f_c'(MPa)})$ should be replaced by $0.19\sqrt{f_c'(ksi)}$ $(0.5\sqrt{f_c'(MPa)})$.
4. The equivalent rectangular concrete compressive stress block of $0.85f_c'$ (Section 5.7.2.2) in the LRFD Specifications should be replaced by $\alpha_1 f_c'$ where α_1 is defined as follows:

$$\alpha_1 = \begin{cases} 0.85 & for\ f_c' \le 10ksi \\ 0.85 - 0.02(f_c' - 10) \ge 0.75 & for\ f_c' > 10ksi \end{cases} \quad (f_c' \text{ in ksi})$$
$$\alpha_1 = \begin{cases} 0.85 & for\ f_c' \le 69MPa \\ 0.85 - 0.003(f_c' - 69) \ge 0.75 & for\ f_c' > 69MPa \end{cases}$$
$$(f_c' \text{ in MPa}) \tag{3-5}$$

   where α_1 is the ratio of equivalent rectangular concrete compressive stress block intensity to the specified compressive strength of concrete, f_c'.
5. A new section (Section 5.7.3.2.6) should be added to the LRFD Specifications that addresses the nominal flexural resistance, M_n, of prestressed HSC girders with NSC deck, in which the neutral axis is located below the deck and within the prestressed girder. The nominal flexural resistance, M_n, should be determined by using LRFD Specifications Equation 5.7.3.2.2-1, based on the concrete compressive strength of the deck.
6. The minimum area of prestressed and non-prestressed longitudinal reinforcement for non-composite compression components required by the LRFD Specifications (Equation 5.7.4.2-3 and Equation 3-6) should be replaced by Equation 3-7:

$$\frac{A_s f_y}{A_g f_c'} + \frac{A_{ps} f_{pu}}{A_g f_c'} \ge 0.135 \tag{3-6}$$

$$\frac{A_s}{A_g}+\frac{A_{ps}f_{pu}}{A_g f_y}\geq 0.135\frac{f_c'}{f_y}\text{ but not greater than }0.0225 \qquad (3\text{-}7)$$

where f_c' is the concrete compressive strength, A_{ps} is the area of prestressing steel, f_{pu} is the specified tensile strength of prestressing steel, A_s and f_y are the area and yield strength of mild tension steel, respectively, and A_g is the gross area of the section.

7. The in-place concrete strength, $0.85f_c'$, for the concrete contribution to the factored axial resistance of concrete compressive components in the LRFD Specifications (Equations 5.7.4.4-2, 5.7.4.4-3, and 5.7.4.5-2) should be replaced by $k_c f_c'$ where k_c is defined as follows:

$$k_c=\begin{cases}0.85 & \text{for } f_c'\leq 10\,ksi\\ 0.85-0.02(f_c'-10)\geq 0.75 & \text{for } f_c'>10\,ksi\end{cases}\quad(f_c' \text{ in ksi})$$

$$k_c=\begin{cases}0.85 & \text{for } f_c'\leq 69\,MPa\\ 0.85-0.003(f_c'-69)\geq 0.75 & \text{for } f_c'>69\,MPa\end{cases}$$

$$(f_c' \text{ in MPa}) \qquad (3\text{-}8)$$

where k_c is the ratio of in-place concrete compressive strength to the specified compressive strength of concrete, f_c'.

CHAPTER 4

Conclusions and Future Research

4.1 Conclusions

Based on the research conducted to extend the current AASHTO LRFD Bridge Design Specifications to include HSC up to 18 ksi (124 MPa), the following conclusions can be drawn:

- Comparisons of the compressive strengths of the 7-day moist-cured and the continuously moist-cured specimens suggested that, for HSC, moist curing beyond 7 days does not result in any significant increase in strength because of the low permeability of HSC and the short time required for the capillary pores to be blocked.
- The equation for modulus of elasticity specified by the LRFD Specifications over-estimated the elastic modulus for all specimens. A new equation is proposed for the modulus of elasticity of concrete up to 18 ksi (124 MPa).
- Test results suggest that the current lower bound of the LRFD Specifications using $0.24\sqrt{f_c'(ksi)}$ $(0.62\sqrt{f_c'(MPa)})$ overestimates the modulus of rupture for HSC. A better predictive equation, $f_r = 0.19\sqrt{f_c'(ksi)}$ $(f_r = 0.5\sqrt{f_c'(MPa)})$, is proposed for HSC up to 18 ksi (124 MPa).
- Poisson's ratio of 0.2 was found to be acceptable for concrete compressive strengths up to 18 ksi (124 MPa).
- The creep and shrinkage relationships specified by the LRFD Specifications were found to be applicable for HSC except that the time-development correction factor (k_{td}) would produce negative values in the first few days if concrete strengths were greater than 15 ksi (103 MPa). Accordingly, a new time-development correction factor was developed to overcome the anomaly associated with the current time-development correction factor.
- The ultimate concrete compressive strain value of 0.003 specified by the LRFD Specifications is acceptable for HSC up to 18 ksi (124 MPa).
- The test results, confirmed by other data in the literature, indicate that the stress block parameter α_1 of 0.85 should be reduced when the compressive strength of concrete increases beyond 10 ksi (69 MPa). A new relationship is recommended for the parameter α_1 for concrete compressive strengths up to 18 ksi (124 MPa).
- The current value of the stress block parameter β_1 specified by LRFD Specifications is appropriate for HSC up to 18 ksi (124 MPa).
- For HSC beams and beam-columns, prediction of nominal flexural resistance using the current LRFD Specifications is less conservative and less accurate. Using the proposed stress block parameter α_1 would improve the prediction.
- The crack width specified for Class 1 exposure condition in the LRFD Specifications safely exceeds the measured crack widths for most of the beams tested in this study.
- The current LRFD Specifications underestimates the beam deflection at service load for all tested specimens in this project. However, the discrepancy is within the commonly acknowledged limit for NSC.
- For concrete compressive strengths beyond 10 ksi (69 MPa), use of the constant 0.85 as the ratio of in-place concrete strength to the cylinder strength overestimates the load carrying capacity for concentrically loaded columns. A new relationship for a parameter k_c in lieu of the constant 0.85 is proposed for HSC up to 18 ksi (124 MPa).
- Test results of eccentrically loaded columns show that using the proposed parameter α_1 produces improved comparison of the predictions and the test results.
- The maximum tie spacing and the minimum volumetric ratio of spiral required by the LRFD Specifications are applicable for reinforced concrete columns with compressive strengths up to 18 ksi (124 MPa).
- For design purposes, the 20-percent reduction in the axial load capacity of the tied columns with HSC to account for unintentional eccentricity is reasonable and conservative.
- It is adequate to use the proposed modulus of rupture to predict the cracking moment of prestressed HSC girders for concrete strengths up to 18 ksi (124 MPa).

- The current LRFD Specifications requires excessively high levels of minimum reinforcement ratio for compression members for concrete compressive strengths over 10 ksi (69 MPa). Based on the performed analysis using the proposed equation for E_c and the current relationship specified by the LRFD Specifications, a new relationship is proposed for the minimum reinforcement ratio for compression members with concrete compressive strengths up to 18 ksi (124 MPa).
- Based on the test results of prestressed concrete girders, the LRFD Specifications may be used to determine transfer length of prestressed HSC girders with concrete compressive strength up to 18 ksi (124 MPa).
- For composite girder section in which the neutral axis is located below the deck and within the prestressed high-strength concrete girder, the nominal flexural resistance may be determined conservatively based on the concrete compressive strength of the deck.
- For prestressed HSC girder section without a composite deck, the nominal flexural strength can be determined using the LRFD Specifications procedure and the proposed relationship for α_1 for concrete strengths up to 18 ksi (124 MPa).

4.2 Future Research

The number of tests performed to evaluate the stress-strain distribution, shrinkage, and creep behavior under controlled environment, and cracking and deflection of HSC members is limited for concrete compressive strengths over 16 ksi (110 MPa). More studies with concrete compressive strengths beyond 16 ksi (110 MPa) would enhance the confidence level of the various proposed equations of the current research.

More tests should be conducted to evaluate the long-term behavior of HSC under field conditions as opposed to laboratory studies, including the differences in curing and size effect of structural members.

To maximize the benefits of HSC, studies should be conducted on the use of high-strength reinforcement.

To fully exploit the benefits of HSC, more studies are needed for ductility of HSC members and the use of HSC in seismic zones. In addition, the effects of repeated loading and reversed cyclic loading on the behavior of HSC members should also be examined.

References

1. American Association of State Highway and Transportation Officials, "AASHTO LRFD Bridge Design Specifications—Third Edition including 2005 and 2006 Interim Revisions." Washington, DC (2004).
2. ACI Committee 318, "Building Code Requirements for Structural Concrete (ACI 318-05) and Commentary (318R-05)." American Concrete Institute, Farmington Hills, MI (2005) 430 pp.
3. Tadros, M. K., Al-Omaishi, N., Seguirant, S. J., and Gallt, J. G., "Prestress Losses in Pretensioned High-Strength Concrete Bridge Girders." *NCHRP Report 495*, Transportation Research Board, Washington, DC (2003) 63 pp.
4. AASHTO T 22, "Compressive Strength of Cylindrical Concrete Specimens." American Association of State Highway and Transportation Officials, Washington, DC (2004).
5. ASTM C 39, "Test Method for Compressive Strength of Cylindrical Concrete Specimens." ASTM International, Conshohocken, PA.
6. ASTM C 469, "Test Method for Splitting Tensile Strength of Cylindrical Concrete Specimens." ASTM International, Conshohocken, PA.
7. American Concrete Institute Committee 363, "State-of-the-Art Report on High-Strength Concrete (ACI 363R-92)." Detroit, MI (1992 - Revised 1997) 55 pp.
8. AASHTO T 97, "Standard Method of Test for Flexural Strength of Concrete." American Association of State Highway and Transportation Officials, Washington, DC (2004).
9. Légeron, F., and Paultre, P., "Prediction of Modulus of Rupture of Concrete." *ACI Materials Journal*, Vol. 97, No. 2 (2000) pp. 193–200.
10. Paultre, P., and Mitchell, D., "Code Provisions for High-Strength Concrete – An International Perspective." *Concrete International*, Vol. 25, No. 5 (May 2003) pp. 76–90.
11. Mokhtarzadeh, A., and French, C., "Mechanical Properties of High-Strength Concrete with Consideration for Precast Applications." *ACI Materials Journal*, Vol. 97, No. 2 (2000) pp. 136–147.
12. Li, B., "Strength and Ductility of Reinforced Concrete Members and Frames Constructed Using High-Strength Concrete." *Research Report No. 94-5*, Department of Civil Engineering, University of Canterbury, Christchurch, New Zealand (1994) 389 pp.
13. Noguchi Laboratory Data, Department of Architecture, University of Tokyo, Japan, (http://bme.t.u-tokyo.ac.jp/index_e.html).
14. Komendant, J., Nicolayeff, V., Polivka, M., and Pirtz, D., "Effect of Temperature, Stress Level, and Age at Loading on Creep of Sealed Concrete." *Special Publication 55*, American Concrete Institute (August 1978) pp. 55–82.
15. Perenchio, W. F., and Klieger, P., "Some Physical Properties of High-Strength Concrete." *Research and Development Bulletin RD056.01T*, Portland Cement Association (1978) 6 p.
16. Carrasquillo, R. L., Nilson, A. H., and Slate, F. O., "Properties of High-Strength Concrete Subject to Short-Term Loads." *ACI Structural Journal*, Vol. 78, No. 3 (May 1981) pp. 171–178.
17. Swartz, S. E., Nikaeen, A., Narayan Babu, H. D., Periyakaruppan, N., and Refai, T. M. E., "Structural Bending Properties of Higher Strength Concrete." *Special Publication 87*, American Concrete Institute (September 1985) pp. 145–178.
18. Jerath, S., and Yamane, L. C., "Mechanical Properties and Workability of Superplasticized Concrete." *Cement Concrete and Aggregates*, Vol. 9, No. 1 (1987) pp. 12–19.
19. Radain T. A., Samman, T. A., and Wafa, F. F., "Mechanical Properties of High Strength Concrete." *Proceedings of Utilization of High-Strength Concrete Symposium*, Lillehammer, Norway (June 20-23, 1993) pp. 1209–1216.
20. Iravani, S., "Mechanical Properties of High-Strength Concrete." *ACI Materials Journal*, Vol. 93, No. 5 (September-October 1996) pp. 416–426.
21. ASTM C 157, "Standard Test Method for Length Change of Hardened Hydraulic-Cement Mortar and Concrete." ASTM International, Conshohocken, PA.
22. Hognestad, E., Hanson, N. W., and McHenry, D., "Concrete Stress Distribution in Ultimate Strength Design." *ACI Journal*, Vol. 52, No. 4 (December 1955) pp. 455-479.
23. Nedderman, H., "Flexural Stress Distribution in Very-High Strength Concrete." *M.S. Thesis*, Civil Engineering Department, University of Texas at Arlington, Arlington, TX (December 1973) 182 pp.
24. Kaar, P. H., Hanson, N. W., and Capell, H. T., "Stress-Strain Characteristics of High Strength Concrete." *Special Publication 55*, American Concrete Institute (August 1978) pp. 161–185.
25. Kaar, P. H., Fiorato, A. E., Carpenter, J. E., and Corely, W. G., "Limiting Strains of Concrete Confined by Rectangular Hoops." *Research and Development Bulletin RD053.01D*, Portland Cement Association (1978) 12 pp.
26. Pastor, J. A., "High-Strength Concrete Beams." *Ph.D. Thesis*, Department of Civil Engineering, Cornell University, Ithaca, NY (January 1986) 277 pp.
27. Schade, J. E., "Flexural Concrete Stress in High Strength Concrete Columns." *M.S. Thesis*, Civil Engineering Department, the University of Calgary, Calgary, Alberta, Canada (September 1992) 156 pp.

28. Ibrahim, H. H. H., "Flexural Behavior of High-Strength Concrete Columns." *Ph.D. Thesis*, Department of Civil and Environmental Engineering, University of Alberta, Alberta, Edmonton, Alberta, Canada (1994) 221 pp.
29. Tan, T. H., and Nguyen, N., "Flexural Behavior of Confined High-Strength Concrete Columns." *ACI Structural Journal*, Vol. 102, No. 2 (March 2005) pp. 198–205.
30. Rashid, M.A., and Mansur, M.A., "Reinforced High-strength Concrete Beams in Flexure." *ACI Structural Journal*, Vol. 102, No. 3 (May-June 2005) pp. 462–471.
31. Ashour, S.A., " Effect of Compressive Strength and Tensile Reinforcement Ratio on Flexural Behavior of High-Strength Concrete Beams." *Engineering Structures*, Vol. 22, No. 5 (2000) pp. 413-423.
32. Lin, C-Hung, "Flexural Behavior of High Strength Fly Ash Concrete Beams." *Journal of the Chinese Institute of Engineers*, Vol. 15, No. 1 (January 1992) pp. 85–92.
33. Lambotte, H., and Taerwe, L.R. "Deflection and Cracking of High-strength Concrete Beams and Slabs." *Special Publication 121*, American Concrete Institute (1990) pp. 109–128.
34. Paulson, K.A., Nilson, A. H., and Hover, K. C. "Long-term Deflection of High-Strength Concrete Beams." *ACI Materials Journal*, Vol. 88, No. 2 (March-April 1991) pp. 197–206.
35. Shin, S., Ghosh, S. K., and Moreno, J., "Flexural Ductility of Ultra-High-Strength Concrete Members." *ACI Structural Journal*, Vol. 86, No. 4 (1989) pp. 394–400.
36. Pastor, J.A., Nilson, A.H., and Slate, F.O., "Behavior of High-strength Concrete Beams." *Research Report No. 84-3*, Department of Structural Engineering, Cornell University, Ithaca, NY (1984) 331 pp.
37. Frosch, R. J., "Flexural Crack Control in Reinforcement Concrete." Special Publication 204, American Concrete Institute (2001) pp. 135–153.
38. Cusson, D., and Paultre, P., "High-Strength Concrete Columns Confined by Rectangular Ties." *ASCE Journal of Structural Engineering*, Vol. 120, No. 3 (1994) pp. 783–804.
39. Sheikh, S.A., and Uzumeri, S.M., "Strength and Ductility of Tied Concrete Columns." *ASCE Journal of Structural Engineering*, Vol. 106, No. 5 (1980) pp. 1079-1102.
40. Saatcioglu, M., and Razvi, S.R., "High-Strength Concrete Columns with Square Sections under Concentric Compression." *ASCE Journal of Structural Engineering*, Vol. 124, No. 12 (1998) pp. 1438–1447.
41. Sharma, U. K., Bhargava, P., and Kaushik, S. K., "Behavior of Confined High-Strength Concrete Columns under Axial Compression." *Journal of Advanced Concrete Technology*, Vol. 3, No. 2 (2005) pp. 267–281.
42. Yong, Y., Nour, M. G., and Nawy, E. G., "Behavior of Laterally Confined High Strength Concrete under Axial Loads." *ASCE Journal of Structural Engineering*, Vol. 114, No. 2 (1988) pp. 332–351.
43. Nagashima, T., Sugano, S., Kimura, H., and Ichikawa, A., "Monotonic Axial Compression Test on Ultra-High-Strength Concrete Tied Columns." *Earthquake Engineering Tenth World Conference*, Madrid, Spain, Proceedings (1992) pp. 2983–2988.
44. Issa, M. A., and Tobaa, H., "Strength and Ductility Enhancement in High-Strength Confined Concrete." *Magazine of Concrete Research*, Vol. 46, No. 168 (1994) pp. 177–189.
45. Liu, J., Foster, S. J., and Attard, M. M., "Strength of Tied High-Strength Concrete Columns Loaded in Concentric Compression." *ACI Structural Journal*, Vol. 97, No. 1 (Jan. 2000) pp. 149–156.

Abbreviations and acronyms used without definitions in TRB publications:

AAAE	American Association of Airport Executives
AASHO	American Association of State Highway Officials
AASHTO	American Association of State Highway and Transportation Officials
ACI–NA	Airports Council International–North America
ACRP	Airport Cooperative Research Program
ADA	Americans with Disabilities Act
APTA	American Public Transportation Association
ASCE	American Society of Civil Engineers
ASME	American Society of Mechanical Engineers
ASTM	American Society for Testing and Materials
ATA	Air Transport Association
ATA	American Trucking Associations
CTAA	Community Transportation Association of America
CTBSSP	Commercial Truck and Bus Safety Synthesis Program
DHS	Department of Homeland Security
DOE	Department of Energy
EPA	Environmental Protection Agency
FAA	Federal Aviation Administration
FHWA	Federal Highway Administration
FMCSA	Federal Motor Carrier Safety Administration
FRA	Federal Railroad Administration
FTA	Federal Transit Administration
IEEE	Institute of Electrical and Electronics Engineers
ISTEA	Intermodal Surface Transportation Efficiency Act of 1991
ITE	Institute of Transportation Engineers
NASA	National Aeronautics and Space Administration
NASAO	National Association of State Aviation Officials
NCFRP	National Cooperative Freight Research Program
NCHRP	National Cooperative Highway Research Program
NHTSA	National Highway Traffic Safety Administration
NTSB	National Transportation Safety Board
SAE	Society of Automotive Engineers
SAFETEA-LU	Safe, Accountable, Flexible, Efficient Transportation Equity Act: A Legacy for Users (2005)
TCRP	Transit Cooperative Research Program
TEA-21	Transportation Equity Act for the 21st Century (1998)
TRB	Transportation Research Board
TSA	Transportation Security Administration
U.S.DOT	United States Department of Transportation